TABLE 2. *Survival and differentiation into neurons 28 days after BrdU labeling in the contralateral SGZ and GCL*

	Total BrdU (+) cells/mm^2				
	1 day after BrdU injection	28 days after BrdU injection	Survival rate (%)	BrdU (+) NeuN (+) cells (per total BrdU (+) cells [%])	BrdU (+) GFAP (+) cells (per total BrdU (+) cells [%])
Control (n = 4)	10.1 ± 4.7	9.3 ± 2.5	92.1	73.2 ± 8.7	11.2 ± 10.3
Ischemia (n = 4)	61.2 ± 6.1*	13.4 ± 0.2*	21.9	84.8 ± 3.8	9.6 ± 2.5

* $P < 0.05$ versus control.
BrdU, bromodeoxyuridine; SGZ, subgranular zone; GCL, granular cell layer; GFAP, glial fibrillary acidic protein.

findings (Jin et al., 2001), we could not observe an increase in the number of BrdU-positive cells in the contralateral SVZ after ischemia. Reperfusion or reoxygenation may accelerate proliferation of neural progenitor cells in the SVZ, because Jin et al. used transient MCA occlusion followed by recirculation, but we used a permanent MCA occlusion model. Future study will be required to resolve this disagreement. No increase in BrdU-positive cells in other areas of the contralateral hemisphere would reflect no or very little neurogenesis in the corresponding area of the contralateral side after cerebral infarction.

The second novel finding was the reduced survival of proliferating cells in the SGZ and dentate gyrus after focal ischemia. Although the percentage of neuronal differentiation of BrdU-positive cells was similar between control (73%) and ischemic rats (85%) (Table 2), survival of BrdU-positive cells 28 days after BrdU admin-

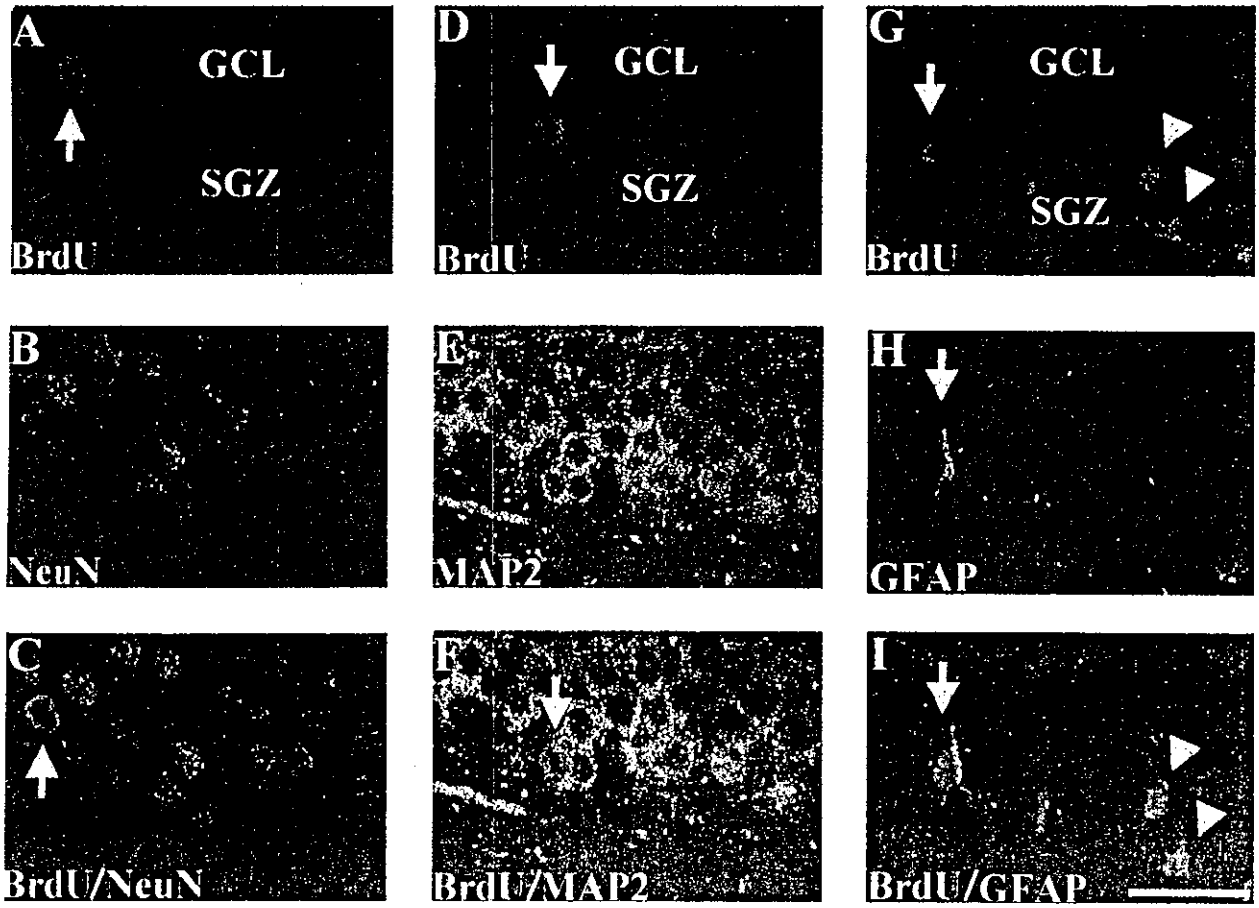

FIG. 7. Neuronal differentiation of newborn cells in the contralateral hippocampus after middle cerebral artery occlusion. Rats received BrdU (BrdU; 50 mg/kg, i.p.) administration three times, 7 days after ischemia, and were killed 28 days after BrdU injection. Left and middle panels: In the subgranular zone (SGZ) and granular cell layer (GCL) (**A–C**; **A:** BrdU, **B:** NeuN, **C:** BrdU/NeuN. **D–F**; **D:** BrdU, **E:** microtubule-associated protein 2 [MAP2], **F:** BrdU/MAP2), an arrow indicates a newborn neuron, which shows BrdU (red in **A** and **D**) and NeuN (green in **B**) or MAP2 (green in **F**) double-positive findings. Right panel (**G–I**; **G:** BrdU, **H:** glial fibrillary acidic protein (GFAP), **I:** BrdU/GFAP): Only a BrdU-positive cell colocalized with GFAP as indicated with an arrow; however, most of BrdU (red) and GFAP (green) immunofluorescence did not colocalize in the SGZ and GCL (I: BrdU/GFAP) as indicated with arrowheads. Bar = 30 μm.

istration was only approximately 20% of that 1 day after labeling in ischemic rats. However, survival of BrdU-positive cells in the control rats (92%) was in fair agreement with the previous findings (Yagita et al., 2001). Although we could not exclude the possibility that disappearance of BrdU-positive cells may indicate fast DNA replication or repair, it is unlikely that BrdU-positive cells divide several times after the next day of labeling, because approximately 80% of BrdU-positive cells expressed immature neuronal marker, DCX, a day after labeling (Fig. 5). Jin et al. (2001) demonstrated contralateral hippocampal neurogenesis in the same model of rat focal ischemia, although they did not examine survival or neuronal differentiation of BrdU-positive cells. Survival and neuronal differentiation of proliferating cells after ischemia may require local factors or a high concentration of growth factors secreted by reactive astrocytes or microglia that reside close to the proliferating cells. Recent evidence demonstrated that proliferation and survival/neuronal differentiation of neural stem cells was determined by distinct factors. For example, exposure to an enriched environment or hippocampus-dependent learning task increased the number of surviving newborn cells (van Praag et al., 1999; Gould et al., 1999) but did not affect proliferation (van Praag et al., 1999). In contrast, adrenalectomy, by reducing corticosteroid levels, increases not only cell proliferation, but also granule cell death in the dentate gyrus through apoptosis (Cameron and McKay, 1999). Recently, we also demonstrated that cell proliferation was preserved, but cell survival was hampered, in the ischemic aged rat hippocampus (Yagita et al., 2001).

Although it remains unclear whether and how increased neurogenesis in the remote area after cerebral infarction may be involved in neuronal plasticity, the molecular mechanisms underlying increased proliferation of neural stem cells, and survival and neuronal differentiation of proliferating cells, are distinct and need to be elucidated to aid development of a novel strategy for enhancing neurogenesis in patients who have had stroke.

Acknowledgments: The authors thank Y. Nishizawa, R. Morimoto, and S. Imoto for their secretarial assistance, and Drs. Arturo Alvarez-Buylla and Kazunobu Sawamoto for their valuable comments on this article.

REFERENCES

Ahmed S, Reynolds BA, Weiss S (1995) BDNF enhances the differentiation but not the survival of CNS stem cell-derived neuronal precursors. *J Neurosci* 15:565–577

Altman J, Das GD (1965) Autoradiographic and histological evidence of postnatal hippocampal neurogenesis in rats. *J Comp Neurol* 124:319–335

Altman J, Das GD (1967) Postnatal neurogenesis in the guinea-pig. *Nature* 214:1098–1101

Arvidsson A, Kokaia Z, Lindvall O (2001) N-methyl-D-aspartate receptor-mediated increase of neurogenesis in adult rat dentate gyrus following stroke. *Eur J Neurosci* 14:10–18

Arsenijevic Y, Weiss S (1998) Insulin-like growth factor-I is a differentiation factor for postmitotic CNS stem cell-derived neuronal precursors: distinct actions from those of brain-derived neurotrophic factor. *J Neurosci* 18:2118–2128

Bernabeu R, Sharp FR (2000) NMDA and AMPA/kainite glutamate receptor modulate dentate neurogenesis and CA3 synapsin-I in normal and ischemic hippocampus. *J Cereb Blood Flow Metab* 20:1669–1680

Bjorklund A, Lindvall O (2000) Self-repair in the brain. *Nature* 403:892–894

Cameron HA, McKay RDG (1999) Restoring production of hippocampal neurons in old age. *Nat Neurosci* 1999;2:894–897

Doetsch F, Caille I, Lim DA, Garcia-Verdugo JM, Alvarez-Buylla A (1999) Subventricular zone astrocytes are neural stem cells in the adult mammalian brain. *Cell* 97:703–716

Eriksson PS, Perfilieva E, Bjork-Eriksson T, Alborn A, Nordborg C, Peterson DA, Gage FH (1998) Neurogenesis in the adult human hippocampus. *Nat Med* 4:1313–1317

Francis F, Koulakoff A, Boucher D, Chafey P, Schaar B, Vinet MC, Friocourt G, McDonnell N, Reiner O, Kahn A, McConnell SK, Berwald-Netter Y, Denoulet P, Chelly J (1999) Doublecortin is a developmentally regulated, microtubule-associated protein expressed in migrating and differentiating neurons. *Neuron* 23:247–256

Gould E, Tanapat P, McEwen BS, Flugge G, Fuchs E (1998) Proliferation of granule cell precursors in the dentate gyrus of adult monkeys is diminished by stress. *Proc Natl Acad Sci U S A* 95:3168–3171

Gould E, Beylin A, Tanapat P, Reeves A, Shors TJ (1999) Learning enhances adult neurogenesis in the hippocampal formation. *Nat Neurosci* 2:260–265

Gu W, Brannstrom T, Wester P (2000) Cortical neurogenesis in adult rats after reversible photothrombotic stroke. *J Cereb Blood Flow Metab* 20:1166–1173

Jin K, Minami M, Lan JQ, Mao XO, Batteur S, Simon RP, Greenberg DA (2001) Neurogenesis in dentate subgranular zone and rostral subventricular zone after focal cerebral ischemia in the rat. *Proc Natl Acad Sci U S A* 98:410–415

Johansson CB, Momma S, Clarke DL, Risling M, Lendahl U, Frisen J (1999) Identification of a neural stem cell in the adult mammalian central nervous system. *Cell* 96:25–34

Kaneko Y, Sakakibara S, Imai T, Suzuki A, Nakamura Y, Sawamoto K, Ogawa Y, Toyama Y, Miyata T, Okano H (2000) Musashi1: an evolutionally conserved marker for CNS progenitor cells including neural stem cells. *Dev Neurosci* 22:139–153

Kee NJ, Preston E, Woitowicz JM (2001) Enhanced neurogenesis after transient global ischemia in the dentate gyrus of the rat. *Exp Brain Res* 136:313–320

Koizumi J, Yoshida Y, Nakazawa T, Ooneda G (1986) Experimental studies of ischemic brain edema. Part 1: a new experimental model of cerebral embolism in rats in which recirculation can be introduced in the ischemic area. *Jpn J Stroke* 8:1–8

Kuhn HG, Winkler J, Kempermann G, Thal LJ, Gage FH (1997) Epidermal growth factor and fibroblast growth factor-2 have different effects on neural progenitors in the adult rat brain. *J Neurosci* 17:5820–5829

Kumihashi K, Uchida K, Miyazaki H, Kobayashi J, Tsushima T, Machida T (2001) Acetylsalicylic acid reduces ischemia-induced proliferation of dentate cells in gerbils. *Neuroreport* 12:915–917

Liu J, Solway K, Messing RO, Sharp FR (1998) Increased neurogenesis in the dentate gyrus after transient global ischemia in gerbils. *J Neurosci* 18:7768–7778

Longa EZ, Weinstein PR, Carlson S, Cummins R (1989) Reversible middle cerebral artery occlusion without craniectomy in rats. *Stroke* 20:84–91

Matsuyama T, Tsuchiyama M, Nakamura H, Matsumoto M, Sugita M (1993) Hilar somatostatin neurons are more vulnerable to an ischemic insult than CA1 pyramidal neurons. *J Cereb Blood Flow Metab* 13:229–234

Nacher J, Crespo C, McEwen BS (2001) Doublecortin expression in the adult rat telencephalon. *Eur J Neurosci* 14:629–644

Pincus DW, Keyoung HM, Harrison-Restelli C, Goodman RR, Fraser RAR, Edgar M, Sakakibara S, Okano H, Nedergaard M, Goldman SA (1998) Fibroblast growth factor-2/brain-derived neurotrophic factor-associated maturation of new neurons generated from adult human subependymal cells. *Ann Neurol* 43:576–585

Reynolds BA, Weiss S (1992) Generation of neurons and astrocytes from isolated cells of the adult mammalian central nervous system. *Science* 255:1707–1710

Roy NS, Wang S, Jiang L, Kang J, Benraiss A, Harrison-Restelli C, Fraser RAR, Couldwell WT, Kawaguchi A, Okano H, Nedergaard M, Goldman SA (2000) *In vitro* neurogenesis by progenitor cells isolated from the adult human hippocampus. *Nat Med* 6:271–277

Sakakibara S, Okano H (1997) Expression of neural RNA-binding proteins in the postnatal CNS: implications of their roles in neuronal and glial cell development. *J Neurosci* 17:8300–8312

Sakakibara S, Imai T, Hamaguchi K, Okabe M, Aruga J, Nakajima K, Yasutomi D, Nagata T, Kurihara Y, Uesugi S, Miyata T, Ogawa M, Mikoshiba K, Okano H (1996) Mouse-musashi-1, a neural RNA-binding protein highly enriched in the mammalian CNS stem cell. *Dev Biol* 176:230–242

Schmidt-Kastner R, Freund TF (1991) Selective vulnerability of the hippocampus in brain ischemia. *Neuroscience* 40:599–636

Seri B, Garcia-Verdugo JM, McEwen BS, Alvarez-Buylla A (2001) Astrocytes give rise to new neurons in the adult mammalian hippocampus. *J Neurosci* 21:7153–7160

States BA, Honkaniemi J, Weinstein PR, Sharp FR (1996) DNA fragmentation and HSP70 protein induction in hippocampus and cortex occurs in separate neurons following permanent middle cerebral artery occlusions. *J Cereb Blood Flow Metab* 16:1165–1175

Takagi Y, Nozaki K, Takahashi J, Yodoi J, Ishikawa M, Hashimoto N (1999) Proliferation of neuronal precursor cells in the dentate gyrus is accelerated after transient forebrain ischemia in mice. *Brain Res* 831:283–287

van Praag H, Christie BR, Sejnowski TJ, Gage FH (1999) Running enhances neurogenesis, learning, and long-term potentiation in mice. *Proc Natl Acad Sci U S A* 96:13427–13431

Yagita Y, Kitagawa K, Ohtsuki T, Takasawa K, Miyata T, Okano H, Hori M, Matsumoto M (2001) Neurogenesis by progenitor cells in the ischemic adult rat hippocampus. *Stroke* 32:1890–1896

Yoshimura S, Takagi Y, Harada J, Teramoto T, Thomas SS, Waeber C, Bakowska J, Breakefield XO, Moskowitz MA (2001) FGF-2 regulation of neurogenesis in adult hippocampus after brain injury. *Proc Natl Acad Sci U S A* 98:5874–5879

Zhang RL, Zhang ZG, Zhang L, Chopp M (2001) Proliferation and differentiation of progenitor cells in the cortex and the subventricular zone in the adult rat after focal cerebral ischemia. *Neuroscience* 105:33–41

Journal of Neuroscience Research 68:226–232 (2002)

Protective Effect of Apolipoprotein E Against Ischemic Neuronal Injury Is Mediated Through Antioxidant Action

Kazuo Kitagawa,[1]* Masayasu Matsumoto,[1,2] Keisuke Kuwabara,[1] Ken-Ichiro Takasawa,[1] Shigeru Tanaka,[1] Tsutomu Sasaki,[1] Kohji Matsushita,[1] Toshiho Ohtsuki,[1] Takehiko Yanagihara,[2] and Masatsugu Hori[1]

[1]Division of Strokology, Departement of Internal Medicine and Therapeutics, Osaka University Graduate School of Medicine, Suita-City, Osaka, Japan

[2]Departement of Clinical Neuroscience, Osaka University Graduate School of Medicine, Suita-City, Osaka, Japan

Recent studies have demonstrated that apolipoprotein E (APOE) deficiency worsened neuronal injuries after transient focal and global cerebral ischemia. However, the molecular mechanism underlying the protective effect of APOE remains uncertain, even though several mechanisms, including excitotoxicty, free radicals, and apoptosis, have been cited as causes of selective neuronal vulnerability in cerebral ischemia. In the present study, we first compared the vulnerability of cultured neurons prepared from APOE-knockout mice upon exposure to glutamate, hydrogen peroxide, and staurosporine. No significant difference in cell viability was observed after exposure to glutamate or staurosporine between APOE-deficient and wild-type mice. However, exposure to hydrogen peroxide significantly increased the level of cell death in APOE-deficient mice compared with that in wild-type mice. After transient forebrain ischemia for 12 min, APOE-deficient mice showed more neuronal death than wild-type mice. Pretreatment of APOE-deficient mice with vitamin E for 2 months markedly reduced neuronal death caused by ischemia. The results suggest that APOE exerted its neuroprotective effect against ischemia through its antioxidant action but not through mitigation of glutamate toxicity or blocking of apoptosis. © 2002 Wiley-Liss, Inc.

Key words: apolipoprotein E; cerebral ischemia; free radicals; vitamin E; neuron

Previous studies have shown that apolipoprotein E (APOE) deficiency worsened histological outcome after transient focal (Laskowtiz et al., 1997) and global (Horsburgh et al., 1999; Sheng et al., 1999) cerebral ischemia and that intraventricular infusion of APOE ameliorated neuronal damage in the caudate nucleus and hippocampal CA2 sector in APOE-deficient mice but not in wild-type mice (Horsburgh et al., 2000). Furthermore, APOE4 transgenic mice developed larger infarcts than APOE3 transgenic mice in a focal cerebral ischemia model (Sheng et al., 1998). These studies supported a protective effect of APOE against ischemic neuronal damage; however, the molecular mechanism underlying the APOE-mediated protection remains unclear. Ischemic neuronal vulnerability after recovery from energy failure may be composed of several factors (Dirnagl et al., 1999). Glutamate toxicity has been believed for more than 10 years to play an essential role in calcium influx into neuronal cytoplasm (Rothmann and Olney, 1986; Hossman, 1994). Subsequent calcium overload has been believed to be the most important factor triggering cell death (Choi, 1995).

Oxidative stress generated by ischemia–reperfusion has also been considered important even before the advent of the concept of excitotoxity (Chan, 2001). Recent studies using transgenic animals, overexpressing superoxide dismutase, supported the involvement of free radicals in ischemic neuronal damage after ischemia–reperfusion (Chan et al., 1998; Kawase et al., 1999). Finally, apoptosis has been examined intensively over the past several years (Linnik et al., 1993; Nitatori et al., 1995; Schulz et al., 1999), although the presence of apoptosis is still controversial (Petito et al., 1997; Colbourne et al., 1999). Other mechanisms, such as inflammation (Kochanek and Hallenbeck, 1992; Mabuchi et al., 2000) and microcirculatory disturbance (del Zoppo, 1994; Kitagawa et al., 1998a), may also contribute to ischemic neuronal vulnerability. In the present study, we tried to clarify which pathway, among glutamate toxicity, oxidative stress, and apoptosis, was effectively blocked by APOE, using cultured neurons

*Correspondence to: Kazuo Kitagawa, MD, Division of Strokology, Departement of Internal Medicine and Therapeutics, Osaka University Graduate School of Medicine (A8), 2-2 Yamadaoka, Suita-City, Osaka 565-0871, Japan. E-mail: kitagawa@medone.med.osaka-u.ac.jp

Received 14 November 2001; Revised 18 January 2002; Accepted 22 January 2002

Published online 11 March 2002 in Wiley InterScience (www.interscience.wiley.com). DOI: 10.1002/jnr.10209

© 2002 Wiley-Liss, Inc.

prepared from APOE-knockout mice and an in vivo model of transient forebrain ischemia.

MATERIALS AND METHODS

Animals

Animals used in the present study were fed standard laboratory chow and given free access to water prior to surgery. All experimental procedures were approved by the Institutional Animal Center Use Committee of the Osaka University Graduate School of Medicine. APOE-knockout mice, originally produced by Zhang et al. (1992), were purchased from the Jackson Laboratory (Bar Harbor, ME) and back-crossed to wild-type C57BL/6 mice (Charles River Inc., Yokohama, Japan) to have genetic backgrounds of the homozygote and wild-type mice. After mating of heterozygotes, we selected the homozygous and wild-type mice by polymerase chain reaction (PCR) amplification of genomic DNA extracted from tails.

Neuron–Glia Mixed Culture

After mating pairs of homozygous mice and of wild-type mice separately, pregnant APOE-knockout and wild-type female mice were used. Primary neuronal cultures containing the hippocampus and cerebral cortex from 15–17 day mouse fetuses were obtained as described previously by Chen and Mattson (1994). Cells were dissociated with papain (Papain Dissociation System; Worthington, Freehold, NJ) and plated onto six-well plates (Falcon, Becton Dickinson and Company, Franklin Lakes, NJ) coated with polyethylenimine at a density of approximately 5.0×10^5 cells/dish in high-glucose Dulbecco's modified Eagle's medium (DMEM; Sigma-Aldrich, Tokyo, Japan) containing 10% fetal calf serum (FCS; Sigma), 100 IU penicillin/ml, and 100 mg of streptomycin sulfate/ml during the first 2 days. Then, the cultures were maintained in Neurobasal Medium (Gibco BRL, Life Technologies, Rockville, MD) containing B27 supplement (Gibco BRL) for the next 3–5 days, and the medium was changed to Neurobasal Medium with B27 supplement but without antioxidants 24 hr before glutamate, hydrogen peroxide, or staurosporine treatment. These cultures contained not only neurons but also astrocytes; the latter constituted approximately 15–20% of the cell population by 7 days.

After 6 or 7 days in culture, cells were treated with glutamate (50 or 100 μM) for 15 min, hydrogen peroxide (5 or 10 μM) for 15 min, or staurosporine (30 or 100 nM) for 1 hr. All chemicals were added directly to the medium. The incubation medium was then changed completely to that without antioxidants. Cell viability was assessed using six-well chambers for each group. Quantitative assessment of neuronal injury was accomplished by measuring lactate dehydrogenase (LDH) activity in the medium 24 hr after exposure to glutamate, hydrogen peroxide, or staurosporine using the Cytotoxicity Detection Kit (Boehringer Manheim, Manheim, Germany). The genotype was again confirmed by immunoblotting of the cell extract using an antibody against APOE (Chemicon, Temecula, CA).

For immunocytochemistry for microtubule-associated protein 2 (MAP2), cells were cultured in two-chamber glass slides and incubated as described above. Twenty-four hours after exposure to glutamate, hydrogen peroxide, or staurosporine, the cells were fixed immediately in 4% paraformaldehyde (PFA) for 15 min and permeabilized with 0.01% Triton X-100. Cells were then incubated with monoclonal anti-MAP2 antibody (1:100; Sigma) for 1 hr at room temperature. The slides were next washed in three changes of phosphate-buffered saline, incubated for 1 hr in a 1:200 dilution of fluorescein isothiocyanate (FITC)-labeled secondary antibody, and evaluated using a confocal microscope. The number of MAP2-positive neurons was counted in a field of 0.01 mm^2.

Transient Forebrain Ischemia

All homozygous and wild-type mice used for transient forebrain ischemia were mature males age at 12–16 weeks weighing 26.6 ± 1.5 g (homozygous; n = 30) and 24.1 ± 2.1 g (wild-type; n = 30), respectively. Fifteen mice in each group were fed a chow diet (CE2; Clea Japan Inc., Osaka, Japan) supplemented with vitamine E (2 g/kg) for 2 months before surgery. Transient forebrain ischemia was created by bilateral common carotid artery (BCCA) occlusion as described previously (Kitagawa et al., 1998b). Each mouse was anesthetized with 2.0% halothane, and anesthesia was maintained with 0.5% halothane by means of an open face mask. A polyacrylamide column for measurement of cortical perfusion by laser Doppler flowmetry (LDF; Unique Medical) was attached to the intact skull with dental cement, 3.5 mm lateral to the bregma. A metal plate-type thermometer was also attached to the skull over the parietal cortex to record skull temperature. Body and skull temperatures were monitored and maintained at 36.0–37.5°C and 35.0–36.5°C, respectively, using a heat lamp. Both common carotid arteries were exposed and occluded with aneurysmal clips. We selected mice that showed less than 12% of baseline cortical microperfusion as measured by LDF during BCCA occlusion for 1 min, based on our previous findings that no patent posterior communicating artery existed on either side, if a mouse showed less than 12% of baseline cortical microperfusion during BCCA occlusion (Kitagawa et al., 1998b). Twenty-four wild-type and twenty-two APOE-knockout mice met the criteria during the first 1 min and were subjected to extended BCCA occlusion for additional 11 min without interruption. Cortical microperfusion by LDF and body and skull temperature were monitored until 15 min of reperfusion. After discontinuation of halothane anesthesia, each mouse was allowed to recover for 2 hr in a separate chamber, where ambient temperature was maintained at 35°C to prevent hypothermia, and they were kept at room temperature afterward. Seven days later, each mouse was killed by an overdose of pentobarbital, and the whole brain was carefully removed and fixed for histological examination by immersion into the alcohol/5% acetic acid solution for 5 hr at 4°C before dehydration and embedding in paraffin, as described previously (Kitagawa et al., 1998b). Tissue sections encompassing the dorsal hippocampus, 5 mm caudal from the frontal pole according to the mouse brain atlas, were examined after staining with hematoxylin-eosin or cresyl violet. For semiquantitative evaluation, the degree of damage was assessed in the CA1–CA3 sector by percentage of damaged cells (Fig. 1): grade 0, no cell damage visible; grade 1, <50% of cells damaged; grade 2, >50% of cells damaged. The length (in millimeters) of the CA1–CA3 sector with each degree of damage was measured, and the mean histological score was calculated as described previously (Kitagawa et al., 1998b) by the

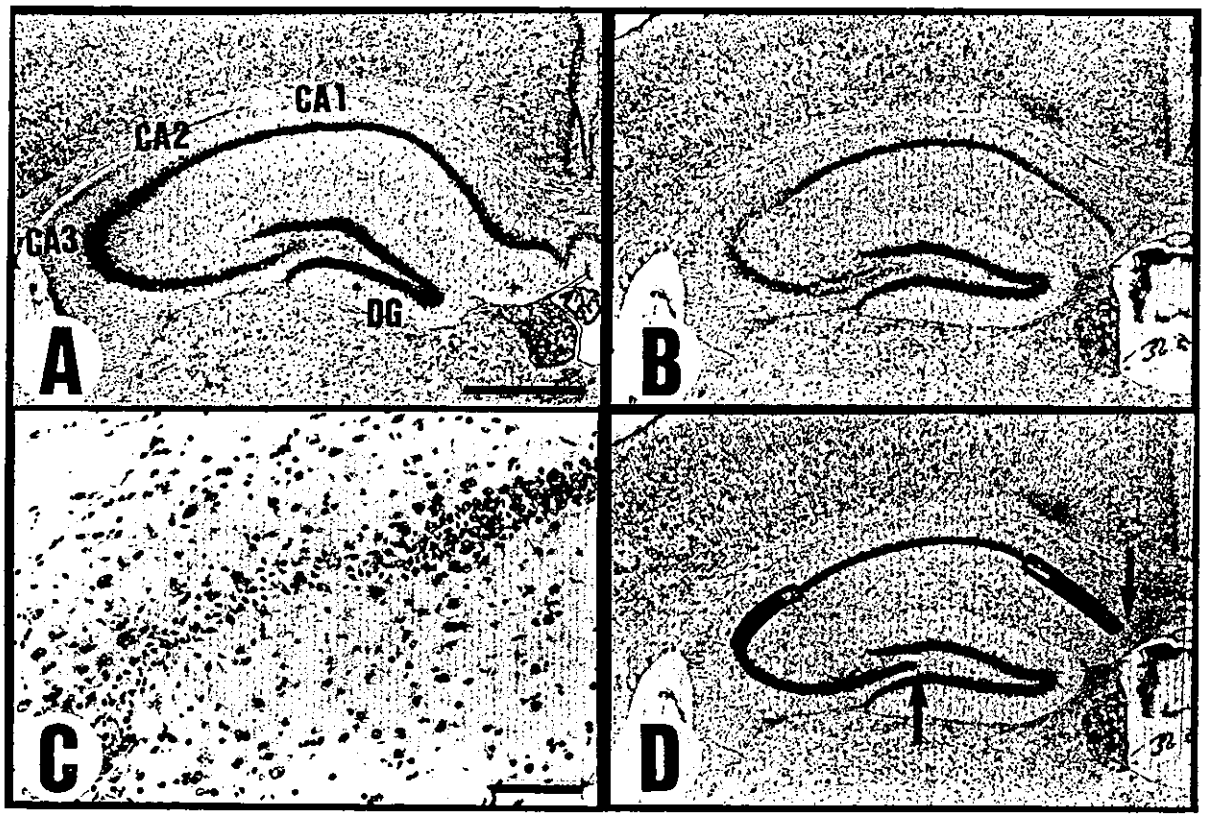

Fig. 1. Semiquantitative evaluation of hippocampal injury. **A:** Normal mouse hippocampus. **B:** Ischemic mouse hippocampus after transient bilateral carotid occlusion for 12 min. **C:** Higher magnification of the lateral segment of CA1, CA2, and part of CA3 in B. Note cell loss in the CA2 and CA3 sectors. **D:** Diagram showing histological grading of B. The thick line denotes the segment with grade 2 damage (>50% of cells are damaged), and the open boxes indicate the segments with grade 1 damage (<50% of cells are damaged); the thin line shows the segment with grade 0 damage (intact). The distance between the two arrows denotes the length from the CA1 to the CA3 sector. Scale bar in A = 0.5 mm for A,B,D; bar in C = 0.1 mm.

following formula: (1 × length with grade 1 + 2 × length with grade 2)/(total length from the CA1 to the CA3 sector).

Statistical Analysis

The results were expressed as mean ± SD. Statistical analysis was performed by one-way ANOVA, followed by Scheffe's test. $P < 0.05$ was considered statistically significant.

RESULTS

Cell Cultures

Western blot analysis of cell extract from wild-type mice showed a 34 kDa band. There was no band in the knockout mice. After medium change, percentage release of LDH after 24 hr was 19.3% ± 1.9% in wild-type mice (n = 6) and 22.6% ± 0.7% in APOE-knockout mice (n = 4), and no significant difference was observed between them (Fig. 2). No significant difference in cell viability was found after exposure to either glutamate (at 50 μM, percentage release of LDH: 44.4% ± 10.1% in wild-type mice, n = 6, and 43.6% ± 9.4% in APOE-knockout

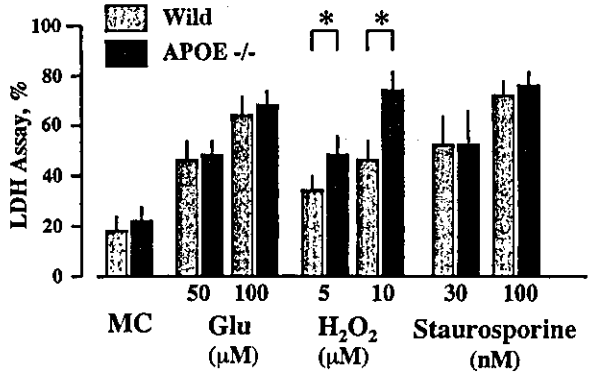

Fig. 2. Neuronal cell death assessed by LDH release 24 hr after exposure to glutamate (Glu, 50 or 100 μM) or hydrogen peroxide (H_2O_2, 5 or 10 μM) for 15 min or staurosporine (30 or 100 nM) for 1 hr in the primary culture prepared from wild-type and APOE-knockout mice. *$P < 0.05$ between the two types of mice. MC, medium change only.

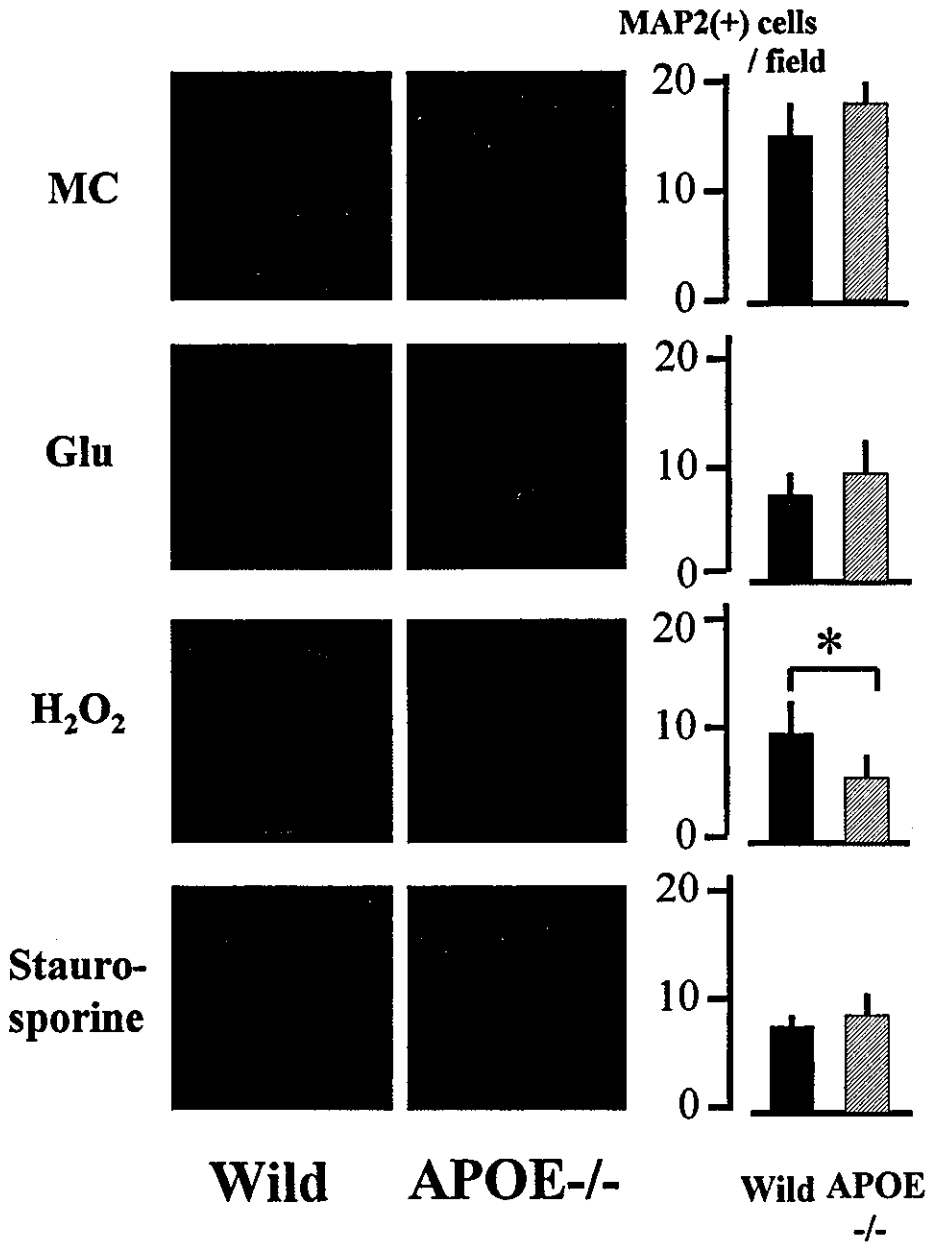

Fig. 3. Immunocytochemistry for MAP2 in cultured neurons from wild-type and APOE-knockout mice. MC, medium change only; Glu, glutamate treatment (100 μM). Cytoplasms and processes of cultured cells are MAP2-positive in neurons prepared from both types of mice. The right panels show the number of MAP2-positive neurons in the field of 0.01 mm^2. The number of MAP2-positive neurons decreased similarly after exposure to glutamate and staurosporine (100 nM) in both wild-type and APOE-knockout mice, but more marked reduction of MAP2-positive neurons was observed in APOE-knockout mice after exposure to hydrogen peroxide (10 μM). $*P <$ 0.05 between two types of mice.

mice, n = 6; at 100 μM, 64.4% ± 7.7% in wild-type mice, n = 6, and 65.2% ± 3.2% in APOE-knockout mice, n = 6) or staurosporine (at 30 nM, percentage release of LDH: 50.8% ± 10.4% in wild-type mice, n = 5, and 49.6% ± 12.1% in APOE-knockout mice, n = 5; at 100 nM, 70.5% ± 5.5% in wild-type mice, n = 5, and 74.5% ± 2.0% in APOE-knockout mice, n = 5). However, exposure to hydrogen peroxide caused significant worsening of neuronal injury in APOE-knockout mice (percentage release of LDH: 46.3% ± 9.4% at 5 μM, and 74.3% ± 8.0% at 10 μM, n = 5 each) compared with that in wild-type mice (34.4% ± 8.4% at 5 μM, and 42.2% ± 10.6% at 10 μM, n = 5 each). The number of MAP2-positive neurons decreased after exposure to glutamate, hydrogen peroxide, and staurosporine compared with that after medium change alone in both wild-type and APOE-knockout mice (Fig. 3). The degree of decrease in MAP2-positive cells after exposure to glutamate and hydrogen peroxide was similar in both types; however, significant decrease in MAP2-positive cells was observed after exposure to hydrogen peroxide in APOE-knockout mice from in wild-type mice (Fig. 3).

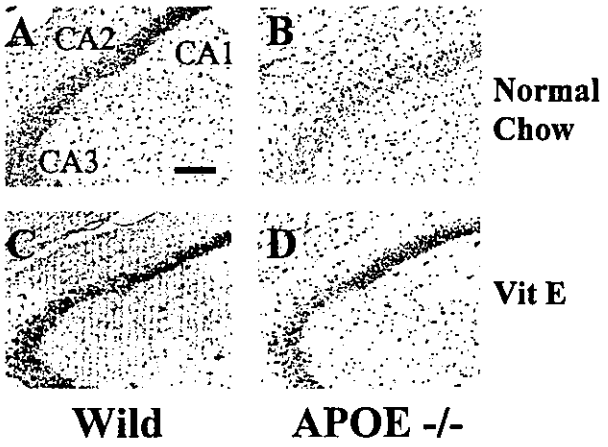

Fig. 4. Hippocampal injury after ischemia in wild-type and APOE-knockout mice fed with normal chow or vitamin E supplementation. In the wild-type mouse fed normal chow, cell loss was observed in the CA2 sector, but, in the APOE-knockout mouse fed normal chow, extensive cell loss occurred in the CA2 and CA3 sector. In both types of mice with vitamin E supplementation, scattered cell loss was observed in the CA2 sector. VitE, vitamin E supplementation. Scale bar = 50 μm.

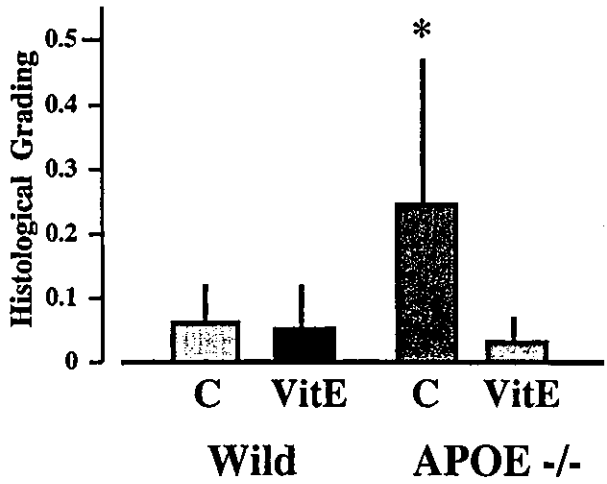

Fig. 5. Semiquantitatve assessment of ischemic neuronal damage in the hippocampus after transient global ischemia for 12 min. The histological grade was calculated by dividing the integration of each grading and its length by the total length of the CA1–CA3 sector. There was no difference in wild-type mice after VitE supplementation, but neuronal damage seen in APOE-knockout mice with normal chow was markedly reduced by vitamin E supplementation. C, normal chow; VitE, vitamin E supplementation. $*P < 0.02$ vs. the other three groups.

Hippocampal Injury After Transient Forebrain Ischemia

Residual cortical microperfusion during BCCA occlusion was about 5% of the baseline, but cortical microperfusion jumped to 70–130% of the baseline after reperfusion in both wild-type and APOE-knockout mice with or without vitamin E supplementation. Body and skull temperature were maintained similarly between two groups. One of twenty-four wild-type and three of twenty-two APOE-knockout mice died during reperfusion. In the normal-chow group, APOE-knockout mice showed a higher degree of neuronal damage after ischemia than wild-type mice (Fig. 4). After vitamin E supplementation, only scattered cell death in the CA2 was observed in both types. In the normal-chow group, the mean histological score for wild-type mice (0.052 ± 0.071; $n = 12$) was significantly less than that for APOE-knockout mice (0.232 ± 0.229; $n = 9$; $P < 0.02$; Fig. 5). However, vitamin E supplementation markedly reduced ischemic injury in APOE-knockout mice (0.020 ± 0.033, $n = 10$; $P < 0.01$ vs. normal-chow group; Fig. 5).

DISCUSSION

APOE protein was found to be expressed in reactive astrocyte, degenerating neurons, and macrophages after cerebral ischemia (Hall et al., 1995; Kida et al., 1995; Horsburgh and Nicoll, 1996; Ishimaru et al., 1996; Ali et al., 1996; Kitagawa et al., 2001), and several studies have supported the protective role of endogenous APOE against ischemic brain injury by using APOE-knockout mice (Laskowitz et al., 1997; Sheng et al., 1999; Horsburgh et al., 1999). However, the mechanism inducing the neuroprotective effect of APOE remains unclear. Selective neuronal vulnerability has been extensively investigated, where excitotoxicity, oxidative stress, and apoptosis have been considered crucial or very important. Therefore, we used the primary culture system to examine which insult was more toxic to cultured neurons derived from APOE-knockout mice after exposure to glutamate, hydrogen peroxide, or staurosporine.

Staurosporine is an inhibitor of protein kinase A and can induce apoptosis in cultured neurons (Koh et al., 1995). Our study clearly demonstrated that cultured neurons derived from APOE-knockout mice were more vulnerable after exposure to hydrogen peroxide. The lack of difference between APOE-knockout and wild-type mice after exposure to glutamate was in agreement with Lendon et al. (2000), who demonstrated no effect of endogenous APOE on neuronal cell death caused by exposure to N-methyl-D-aspartic acid. However, experiments with transgenic mice or gene transfer with the human APOE isoform in APOE-knockout mice will be required to confirm the effect of APOE deficiency.

All previous experiments showing protective effect of APOE against cerebral ischemia used *ischemia–reperfusion* models (Laskowitz et al., 1997; Sheng et al., 1999; Horsburgh et al., 1999), where more oxygen radicals occurred compared with *permanent* occlusion models (Peters et al., 1998). Because the antioxidant action and the differential ability of different APOE isoforms to bind 4 hydroxynonenal have been shown for APOE protein in vitro (Miyata and Smith, 1996; Pedersen et al., 2000), we next examined the role of APOE as an antioxidant in cerebral ischemia in

vivo. Because Ramassamy et al. (2001) have demonstrated the reduction of α-tocopherol in the hippocampus of APOE-knockout mice, we also examined the effect of vitamin E supplementation on ischemic neuronal damage in APOE-knockout and wild-type mice. Vitamin E supplementation has been shown to enhance the antioxidative activity in many organs, including brain, and is one of the most commonly used strategies to prevent free radical-mediated pathology in the brain (Hara et al., 1990) and atherosclerotic vessels (Pratico et al., 1998). After transient global ischemia for 12 min, APOE-knockout mice fed normal chow showed more pronounced damage in the hippocampal neurons compared with wild-type mice. This finding was in agreement with the findings in previous studies (Sheng et al., 1999; Horsburgh et al., 1999). Furthermore, vitamin E supplementation markedly mitigated the degree of neuronal damage after ischemia in APOE-knockout mice. Because of the minimal extent of neuronal damage in wild-type mice, we could not assess the effect of vitamin E supplementation in wild-type mice; however, our results support the notion that the difference in the degree of neuronal damage between wild-type and APOE-knockout mice could likely be ascribed to more susceptibility to oxygen radicals in the latter mice.

Although we did not assess lipid peroxidation or levels of oxidative stress in neurons from wild-type and APOE-knockout mice, the finding by Lomnitski et al. (2000) of increased levels of intracellular iron in APOE-knockout mice after head injury supported increased vulnerability to oxygen stress in APOE-knockout mice. Distinct alterations in phospholipid metabolism and phosphoinositide hydrolysis in brains of APOE-knockout mice (De Sarno and Jope, 1998; Lomnitski et al., 1999) may contribute to the effect of APOE deficiency on oxygen stress. In conclusion, our in vitro and in vivo studies demonstrated that the protective effect of APOE previously reported for several ischemia models was mainly ascribable to its antioxidant action.

ACKNOWLEDGMENTS

The authors thank Mr. Nobuo Katsube of Ono Pharmaceutical Company for technical assistance, and Miss R. Morimoto and Miss S. Imoto for secretarial assistance. The present study was supported in part by a Grant-in-aid for Scientific Research on Priority Areas (A) in Japan.

REFERENCES

Ali SM, Dunn E, Oostveen JS, Hall ED, Carter DB. 1996. Induction of apolipoprotein E mRNA in the hippocampus of the gerbil after transient global ischemia. Mol Brain Res 38:37–44.

Chan PH. 2001. Reactive oxygen radicals in signaling and damage in the ischemic brain. J Cereb Blood Flow Metab 21:2–14.

Chan PH, Kawase M, Murakami K, Chen SF, Li Y, Calgui B, Reola L, Carlson E, Epstein CJ. 1998. Overexpression of SOD1 in transgenic rats protects vulnerable neurons against ischemic damage after global cerebral ischemia and reperfusion. J Neurosci 18:8292–8299.

Chen B, Mattson MP. 1994. NT-3 and BDNF protect CNS neurons against metabolic/excitotoxic insults. Brain Res 640:56–67.

Choi DW. 1995. Calcium: still center-stage in hypoxic–ischemic neuronal death. Trends Neurosci 18:58–60.

Colbourne F, Sutherland GR, Auer RN. 1999. Electron microscopic evidence against apoptosis as the mechanism of neuronal death in global ischemia. J Neurosci 19:4200–4210.

De Sarno P, Jope RS. 1998. Phosphoinositide hydrolysis activated by muscarinic or glutamatergic, but not adrenergic, receptors is impaired in ApoE-deficient mice and by hydrogen peroxide and peroxynitrite. Exp Neurol 152:123–128.

del Zoppo GJ. 1994. Microvascular changes during cerebral ischemia and reperfusion. Cerebrovasc Brain Metab Rev 6:47–96.

Dirnagl U, Iadecolla C, Moskowitz MA. 1999. Pathobiology of ischemic stroke: an integrated view. Trends Neurosci 22:391–397.

Hall ED, Oostveen JA, Dunn E, Carter DB. 1995. Increased amyloid protein precursor and apolipoprotein E immunoreactivity in the selectively vulnerable hippocampus following transient forebrain ischemia in gerbils. Exp Neurol 135:17–27.

Hara H, Kato H, Kogure K. 1990. Protective effect of alpha-tocopherol on ischemic neuronal damage in the gerbil hippocampus. Brain Res 510: 335–338.

Horsburgh K, Nicoll JAR. 1996. Selective alterations in the cellular distribution of apolipoprotein E immunoreactivity following transient cerebral ischemia in the rat. Neuropathol Appl Neurobiol 22:342–349.

Horsburgh K, Kelly S, McCulloch J, Higgins GA, Roses AD, Nicoll JA. 1999. Increased neuronal damage in apolipoprotein E-deficient mice following global ischemia. Neuroreport 10:837–841.

Horsburgh K, McCulloch J, Nilsen M, McCracken E, Large C, Roses AD, Nicoll JAR. 2000. Intraventricular infusion of apolipoprotein E ameliorates acute neuronal damage after global cerebral ischemia in mice. J Cereb Blood Flow Metab 20:458–462.

Hossman KA. 1994. Glutamate-mediated injury in focal cerebral ischemia: the excitotoxin hypothesis revised. Brain Pathol 4:23–36.

Ishimaru H, Ishikawa K, Ohe Y, Takahashi A, Maruyama Y. 1996. Cystatin C and apolipoprotein E immunoreactivities in CA1 neurons in ischemic gerbil hippocampus. Brain Res 709:155–162.

Kawase M, Murakami K, Fujimura M, Morita-Fujimura Y, Gasche Y, Kondo T, Scott RW, Chan PH. 1999. Exacerbation of delayed cell injury after transient global ischemia in mutant mice with CuZn superoxide dismutase deficiency. Stroke 30:1962–1968.

Kida E, Pluta R, Lossinsky AS, Golabek AA, Choi-Miura NH, Wisniewski HM, Mossakowski MJ. 1995. Complete cerebral ischemia with short term survival in rat induced by cardiac arrest. II. Extracellular and intracellular accumulation of apolipoproteins E and J in the brain. Brain Res 674:341–346.

Kitagawa K, Matsumoto M, Mabuchi T, Yagita Y, Ohtsuki T, Hori M, Yanagihara T. 1998a. Deficiency of intercellular adhesion molecule 1 attenuates microcirculatory disturbance and infarction size in focal cerebral ischemia. J Cereb Blood Flow Metab 18:1336–1345.

Kitagawa K, Matsumoto M, Tsujimoto Y, Ohtsuki T, Kuwabara K, Matsushita K, Yang G, Tanabe H, Martinou JC, Hori M, Yanagihara T. 1998b. Amelioration of hippocampal neuronal damage after global ischemia by neuronal overexpression of BCL-2 in transgenic mice. Stroke 29:2616–2621.

Kitagawa K, Matsumoto M, Kuwabara K, Ohtsuki T, Hori M. 2001. Delayed, but marked, expression of apolipoprotein E is involved in tissue clearance after cerebral infarction. J Cereb Blood Flow Metab 21:1199–1207.

Kochanek PM, Hallenbeck JM. 1992. Polymorphonuclear leukocytes and monocytes/macrophages in the pathogenesis of cerebral ischemia and stroke. Stroke 23:1367–1379.

Koh JY, Wie MB, Gwag BJ, Sensi SL, Canzoniero LM, Demaro J, Csernansky C, Choi DW. 1995. Staurosporine-induced neuronal apoptosis. Exp Neurol 135:153–159.

Laskowitz DT, Sheng H, Bart R, Joyner KA, Roses AD, Warner DS. 1997. Apolipoprotein E deficient mice have increased susceptibility to focal cerebral ischemia. J Cereb Blood Flow Metab 17: 753–758.

Lendon CL, Han BH, Salimi K, Fagan AM, Behrens MI, Muller MC, Holtzman DM. 2000. No effect of apolipoprotein E on neuronal cell death due to excitotoxic and apoptotic agents in vitro and neonatal hypoxic ischemia in vivo. Eur J Neurosci 12:2235–2242.

Linnik MD, Zobrist RH, Hatfield MD. 1993. Evidence supporting a role for programmed cell death in focal cerebral ischemia in rats. Stroke 24:2002–2008.

Lomnitski L, Oron L, Sklan D, Michaelson DM. 1999. Distinct alterations in phospholipid metabolism in brains of apolipoprotein E-deficient mice. J Neurol Res 58:586–592.

Lomnitski L, Nyska A, Shohami E, Chen Y, Michaelson DM. 2000. Increased levels of intracellular iron in the brains of ApoE-deficient mice with closed head injury. Exp Toxicol Pathol 52:177–183.

Mabuchi T, Kitagawa K, Ohtsuki T, Kuwabara K, Yagita Y, Yanagihara T, Hori M, Matsumoto M. 2000. Contribution of microglia/macrophages to expansion of infarction and response of oligodendrocytes after focal cerebral ischemia in rats. Stroke 31:1735–1743.

Miyata M, Smith JD. 1996. Apolipoprotein E allele-specific antioxidant activity and effects of cytotoxicity by oxidative insults and β-amyloid peptides. Nat Genet 14: 55–61.

Nitatori T, Sato N, Waguri S, Karasawa Y, Araki H, Shibanai K, Kominami E, Uchiyama Y. 1995. Delayed neuronal death in the CA1 pyramidal cell layer of the gerbil hippocampus following transient ischemia is apoptosis. J Neurosci 15:1001–1011.

Pedersen WA, Chan SL, Mattson MP. 2000. A mechanism for the neuroprotective effect of apolipoprotein E: isoform-specific modification by the lipid peroxidation product 4-hydroxynonenal. J Neurochem 74:1426–1433.

Peters O, Back T, Lindauer U, Busch C, Megow D, Dreier J, Dirnagl U. 1998. Increased formation of reactive oxygen species after permanent and reversible middle cerebral artery occlusion in the rat. J Cereb Blood Flow Metab 18:196–205.

Petito CK, Torres-Munoz J, Roberts B, Olarte JP, Nowak TS, Pulsinelli WA. 1997. DNA fragmentation follows delayed neuronal death in CA1 neurons exposed to transient global ischemia in the rat. J Cereb Blood Flow Metab 17:967–976.

Pratico D, Tangirala RK, Rader DJ, Rokach J, FitzGerald GA. 1998. Vitamin E suppresses isoprostane generation in vivo and reduces atherosclerosis in ApoE-deficient mice. Nat Med 10:1189–1192.

Ramassamy C, Krzywkowski P, Averill D, Lussier-Cacan S, Theroux L, Christen Y, Davignon J, Poirier J. 2001. Impact of apoE deficiency on oxidative insults and antioxidant levels in the brain. Mol Brain Res 86:76–83.

Rothman SM, Olney JW. 1986. Glutamate and the pathophysiology of hypoxic–ischemia brain damage. Ann Neurol 19:105–111.

Schulz JB, Weller M, Moskowitz MA. 1999. Caspases as treatment targets in stroke and neurodegenerative diseases. Ann Neurol 45:421–429.

Sheng H, Laskowitz DT, Bennet E, Schmechel DE, Bart RD, Sauders AM, Pearlstein RD, Roses AD, Warner DS. 1998. Apolipoprotein E isoform-specific differences in outcome from focal ischemia in transgenic mice. J Cereb Blood Flow Metab 18:361–366.

Sheng H, Laskowitz DT, Mackensen GB, Kudo M, Pearlstein RD, Warner DS. 1999. Apolipoprotein E deficiency worsens outcome from global cerebral ischemia in the mouse. Stroke 30:1118–1124.

Zhang SH, Reddick RL, Piedrahita JA, Maeda N. 1992. Spontaneous hypercholesterolemia and arterial lesions in mice lacking apolipoprotein E. Science 258:468–471.

Journal of Cerebral Blood Flow & Metabolism
22:1004–1009 © 2002 The International Society for Cerebral Blood Flow and Metabolism
Published by Lippincott Williams & Wilkins, Inc., Philadelphia

Assessment of Acetazolamide Reactivity in Cerebral Blood Flow Using Spectral Analysis and Technetium-99m Hexamethylpropylene Amine Oxime

*Masashi Takasawa, †Kenya Murase, ‡Naohiko Oku, *Takuya Yoshikawa, ‡Yasuhiro Osaki, *Masao Imaizumi, §Hiroaki Matsuzawa, §Kouichi Fujino, ‡Kazuo Hashikawa, *Kazuo Kitagawa, *Masatsugu Hori, and *Masayasu Matsumoto

**Division of Strokology, Department of Internal Medicine and Therapeutics, Osaka University Graduate School of Medicine; †Department of Allied Health Sciences, Osaka University Graduate School of Medicine; ‡Department of Nuclear Medicine, Osaka University Graduate School of Medicine; and §Department of Nuclear Medicine, Osaka University Hospital, Osaka, Japan*

Summary: Cerebral blood flow (CBF) can be quantified noninvasively using the brain perfusion index (BPI), determined from radionuclide angiographic data generated with technetium-99m hexamethylpropylene amine oxime (^{99m}Tc-HMPAO). Previously, the BPI has been calculated using graphical analysis (GA); however, the GA method is greatly affected by the first-pass extraction fraction and retention fraction, which are not only variable, but lower in cases with an increased CBF, such as after the administration of acetazolamide. Thus, GA-calculated BPI values (BPI^G) may not reflect the absolute CBF. The objective of this study was to use the spectral analysis of radionuclide angiographic data collected using ^{99m}Tc-HMPAO to examine changes in the BPI after the administration of acetazolamide. We studied the CBF of both cerebral hemispheres in six healthy male volunteers; the BPI was measured at rest and after the intravenous administration of 1 g of acetazolamide. In all participants, an $H_2{}^{15}O$ positron emission tomography (PET) examination was also performed, and the spectral analysis–calculated BPI values (BPI^S) and BPI^G values were compared with the actual CBF measured using $H_2{}^{15}O$ PET ($mCBF^{PET}$). The BPI^S was 1.070 ± 0.051 (mean ± SD) at rest and 1.497 ± 0.098 after acetazolamide; the corresponding BPI^G values were 0.646 ± 0.073 and 0.721 ± 0.107. The BPI^S values were significantly correlated with the $mCBF^{PET}$ values, whereas the BPI^G values were not. According to the BPI^S values, the increase in BPI after the intravenous administration of acetazolamide was 40.1 ± 8.4%, as opposed to an increase of only 11.3 ± 6.5% according to the BPI^G values. These results suggest that the spectral analysis of ^{99m}Tc-HMPAO–generated data yields a more reliable BPI than GA for the quantification of CBF after acetazolamide administration. **Key Words:** Brain perfusion index—Spectral analysis—Graphical analysis—Technetium-99m hexamethylpropylene amine oxime—SPECT.

Several reviews have indicated that the quantitation of cerebral blood flow (CBF) is very important for patient management, especially in patients with cerebrovascular disease (Baron, 2001; Marchal et al., 1999; Hellman and Tikofsky, 1990). Vascular reactivity in the brain after the administration of acetazolamide can have a major impact on the prognosis and therapeutic planning of a case, especially in patients in whom a major artery has been occluded (Kuroda et al., 2001; Vernieri et al., 1999).

Received February 4, 2002; final version received April 15, 2002; accepted April 16, 2002.

Address correspondence and reprint requests to Masashi Takasawa, Division of Strokology, Department of Internal Medicine and Therapeutics, Osaka University Graduate School of Medicine. 2–2, Yamadaoka, Suita City, Osaka, 565-0871, Japan; e-mail: tkswm@medone.med.osaka-u.ac.jp

Matsuda et al. (1992) developed a simple noninvasive method for quantifying brain perfusion using technetium-99m hexamethylpropylene amine oxime (^{99m}Tc-HMPAO) or technetium-99m ethyl cysteinate dimer (^{99m}Tc-ECD) (Matsuda et al., 1995). They calculated the brain perfusion index (BPI) by graphical analysis (GA) of the radionuclide angiographic data (Matsuda et al., 1992, 1995) and obtained a significant regression equation for the relationship between BPI and CBF, as measured by xenon-133 inhalation and single photon emission computed tomography (SPECT) (Matsuda et al., 1992). Regional CBF maps were then acquired using the calculated BPI values and Lassen's linearization correction algorithm (Lassen et al., 1988).

However, since the BPI obtained by GA (BPI^G) is derived from the slope of Gjedde-Patlak plot (Matsuda et

al., 1992, 1995), which is proportional to the product of the first-pass extraction fraction of the tracer, retention fraction [$k_3/(k_2+k_3)$; k_2, back diffusion rate constant; k_3, lipophilic-to-hydrophilic conversion rate constant] and CBF, it does not accurately reflect CBF. The reason for this is that BPI^G is dependent upon the first-pass extraction fraction and retention fraction of the tracer, which generally change according to the CBF. Accordingly, a method for accurately estimating the BPI that is unaffected by the first-pass extraction fraction and retention fraction is needed.

Spectral analysis (SA) was introduced by Cunningham and Jones (1993) to analyze dynamic positron emission tomography (PET) data; this technique provides a spectrum of kinetic components involved in the regional uptake and partitioning of a tracer from blood to tissues and allows a tissue impulse response function to be derived with minimal modeling assumptions (Cunningham and Jones, 1993). Murase et al. (1999) were the first to apply the SA method to dynamic SPECT data acquired with ^{99m}Tc-HMPAO and ^{99m}Tc-ECD, and they emphasized the usefulness of this method, especially in cases where the CBF was elevated.

Acetazolamide is generally used to study the cerebrovascular response and/or to detect areas of misery perfusion (Baron et al., 1981; Hirano et al., 1994). Since CBF studies with ^{99m}Tc-labeled compounds may not reflect the absolute CBF after acetazolamide administration, CBF measurements obtained using ^{99m}Tc-labeled compounds must be corrected after acetazolamide administration. However, there have been no precise reports investigating the changes in the BPI after the intravenous administration of acetazolamide.

The objective of this study was to investigate the degree of increase in both BPI^S and BPI^G values after the intravenous administration of acetazolamide. We also performed $H_2{}^{15}O$ PET examinations at rest and after the intravenous administration of acetazolamide to compare both the SA-calculated BPI values (BPI^S) and BPI^G values with the absolute CBF measured using $H_2{}^{15}O$ PET.

MATERIALS AND METHODS

Theory

Spectral analysis. With SA (Murase et al., 1999), the level of ^{99m}Tc-HMPAO radioactivity in the brain at a given time t [$C^S(t)$] was modeled as a convolution of the blood input function [$C_a(t)$] with a sum of exponential terms, as shown by the following equation:

$$C^S(t) = \sum_{i=0}^{k} \alpha_i \cdot \int_0^t C_a(u) e^{-\beta_i(t-u)} du \qquad (1)$$

where α_i and β_i were constants and assumed to be positive or zero. Since $C^S(t)$ and $C_a(t)$ usually have the same unit (e.g., C_i/mL), α_i has a unit of the reciprocal of time (e.g., min^{-1}). β_i also has a unit of the reciprocal of time (e.g., min^{-1}). The upper limit, k, represents the maximum number of terms to be included in the model and was set at 1,000. The α_i values were determined from Eq. 1 using the level of brain radioactivity measured by radionuclide angiography and the nonnegative least-squares method for β_i, ranging from 0 to 2 min^{-1} with an increment of 0.002 min^{-1}. In the present study, the amount of radioactivity in the aortic arch was taken as in Eq. 1 to maximize the noninvasiveness of the procedure without the need for blood sampling. When $C_a(t)$ was replaced by Dirac's delta function in Eq. 1, the tissue impulse response function [$IRF^S(t)$] was given by the following equation [see Appendix 1]:

$$IRF^S(t) = \sum_{i=0}^{k} \alpha_i \cdot e^{-\beta_i t} \qquad (2)$$

The BPI^S was calculated from the $IRF^S(0)$ as follows:

$$BPI^S = \sum_{i=0}^{k} \alpha_i \qquad (3)$$

where BPI^S is expressed in units of min^{-1}.

Graphical analysis

The BPI^G was calculated as follows (Matsuda et al., 1992):

$$BPI^G = 100 \cdot k_u \cdot \frac{10 \cdot ROI_{aorta}}{ROI_{brain}} \qquad (4)$$

where ROI_{aorta} and ROI_{brain} represent the size of the aortic arch and cerebral hemisphere regions of interest (ROIs), respectively, and where k_u is the unidirectional influx rate of the tracer from the blood to the brain, determined by the slope of the line in the GA within the first 30 seconds after injection (Matsuda et al., 1992). To compare BPI^G with BPI^S, we multiplied the result of Eq. 4 by 0.06 so that the BPI^G and the BPI^S would be expressed in the same units (min^{-1}).

Subjects

Six healthy male volunteers (22 to 27 years old) participated in this study. Informed consent was obtained from each participant after a detailed explanation of the purpose of the study, the risks of irradiation, and the scanning procedures. The study was approved by the Medical Ethics Committee of Osaka University Graduate School of Medicine.

Measurement of brain perfusion index using ^{99m}Tc-HMPAO

For the radionuclide angiography, a bolus of 370 MBq ^{99m}Tc-HMPAO was intravenously injected and sequential imaging was performed while the subject was in a supine position with the front of his body positioned against the gamma camera (RC-2600i; Hitachi Medical Co., Tokyo, Japan) to ensure that both the brain and the heart were within the field of view. The passage of the tracer from the aortic arch to the brain was monitored using a 128 × 128 matrix, and a total of 100 1-second images were obtained using low-energy high-resolution collimators (Matsuda et al., 1992).

To calculate the BPI^S, the raw planar dynamic data were transferred to a workstation (Indigo 2; Silicon Graphics, Mountain View, CA, U.S.A.). ROIs were hand-drawn over the left and right cerebral hemispheres and the aortic arch using the workstation and a software package (Dr. View; Asahi Kasei Joho System Co., Ltd., Tokyo, Japan), as described by Matsuda et al. (1992) (Fig. 1). The BPI^S calculations for the ROIs were performed on the workstation using a software package for BPI analysis developed by Murase (1999).

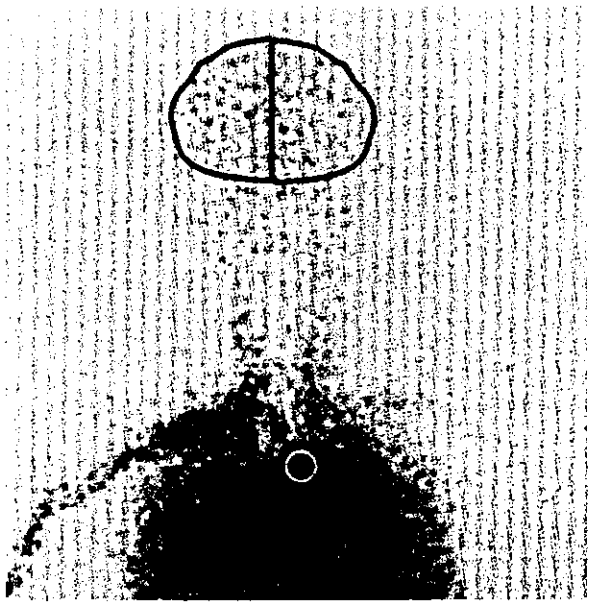

FIG. 1. Example of regions of interest for radionuclide angiographic data obtained using technetium-99m hexamethylpropylene amine oxime.

To measure BPI^G, the raw planar dynamic data were transferred to a Hitachi workstation (RW-3000; Hitachi Medical Co.), and the BPI^G calculations were performed using a software package for Patlak plot analysis (RW-3000; Hitachi Medical Co.) with no filter, as described previously by Matsuda et al. (1992).

Acetazolamide challenges

We measured the BPI at rest [BPI_{rest}] and after acetazolamide administration [BPI_{ACZ}] in all six healthy volunteers. Seven days after the measurement of BPI_{rest}, BPI_{ACZ} was measured 10 minutes after the injection of 1 g of acetazolamide. The rate of BPI increase (% change in BPI) was defined as follows:

$$\% \text{ change in BPI} = 100 \cdot \frac{[BPI_{ACZ}] - [BPI_{rest}]}{[BPI_{rest}]} \quad (5)$$

Measurement of absolute cerebral blood flow using $H_2{}^{15}O$ positron emission tomography

Positron emission tomography data acquisition. BPI and CBF measured using $H_2{}^{15}O$ PET were compared among healthy volunteers. The ^{99m}Tc-HMPAO SPECT at rest and $H_2{}^{15}O$ PET examinations were performed on the same day.

The PET examination was performed using a Headtome V scanner (Shimadzu Corp., Kyoto, Japan) with a spatial resolution of 4.0 mm at full width at half maximum. The subjects were placed in a supine position on a bed in a semidark room and were asked to close their eyes. For the attenuation correction, a transmission scan with a germanium-68/gallium-68 line source was obtained for each patient. The patients received a 36-second intravenous bolus injection of 1,110 MBq $H_2{}^{15}O$ at a flow rate of 30 mL/min through a cannula placed in the antecubital vein. Data were acquired over a scanning period of 160 seconds using a 128 × 128 matrix.

Regional CBF was measured using the $H_2{}^{15}O$ bolus injection (autoradiographic) method (Huang, 1983) while the participants were in a resting state or 10 minutes after the injection of acetazolamide. To evaluate the input function, continuous arterial blood sampling with a catheter needle inserted in the radial artery was performed for 5 minutes at a speed of 5 mL/min, and the ^{15}O radioactivity was concurrently measured using a beta-detector (Shimadzu Corp.).

The transaxial images were reconstructed by the ordered subsets expectation maximization method (Llacer et al., 1993); the final slice thickness was 3.1 mm.

Data analysis of cerebral blood flow measured by $H_2{}^{15}O$ positron emission tomography. The PET data were transferred to a Silicon Graphics workstation. ROIs for the mean CBF measured using $H_2{}^{15}O$ PET ($mCBF^{PET}$) were drawn over the whole left and right cerebral hemispheres of the transaxial image using the "Dr. View" software package (Asahi Kasei Joho System Co., Ltd.) (Nariai et al., 1998). $mCBF^{PET}$ (mL · 100 g^{-1} min^{-1}) was calculated as the mean CBF of five slices, ranging from the basal ganglia level to the upper parietal lobe level.

Statistical analysis

The correlations between BPI^S and BPI^G values and between the BPI and $mCBF^{PET}$ values were assessed by linear regression analysis. The degree of increase in the BPI and $mCBF^{PET}$ values after acetazolamide injection was compared using the Wilcoxon signed rank test. A P value of less than 0.05 was considered significant.

RESULTS

We studied the BPI at rest and 10 minutes after the intravenous administration of 1 g of acetazolamide in six volunteers. The BPI^S was 1.070 ± 0.051 (mean ± SD) at rest and 1.497 ± 0.098 after the administration of acetazolamide; the corresponding BPI^G values were 0.646 ± 0.073 and 0.751 ± 0.107, respectively. The correlations between BPI^S and BPI^G in all studies were not statistically significant (r = 0.285, P = 0.180), with a regression equation of y = 0.120x + 0.530.

The BPI and $mCBF^{PET}$ values are compared in Fig. 2, which shows the relationship between the BPI^S (Fig. 2A) and BPI^G values (Fig. 2B) obtained using ^{99m}Tc-HMPAO and the $mCBF^{PET}$ values. Although the BPI^G and $mCBF^{PET}$ values were not significantly correlated (r = 0.287), the BPI^S and $mCBF^{PET}$ values were significantly correlated (r = 0.940); the regression equation for this relationship was y = 0.017x + 0.364.

We also studied the percentage change in BPI between the values at rest and 10 minutes after acetazolamide administration (Fig. 3). The percentage change in BPI^S after acetazolamide administration (40.1 ± 8.4%) was significantly greater than the change in BPI^G (11.3 ± 6.5%). The $mCBF^{PET}$ was 43.6 ± 2.7 mL · min^{-1} 100 g^{-1} at rest and increased by 55.6 ± 18.4% after the administration of acetazolamide. The percent change in $mCBF^{PET}$ after acetazolamide administration was significantly greater than the change in either BPI^S or BPI^G.

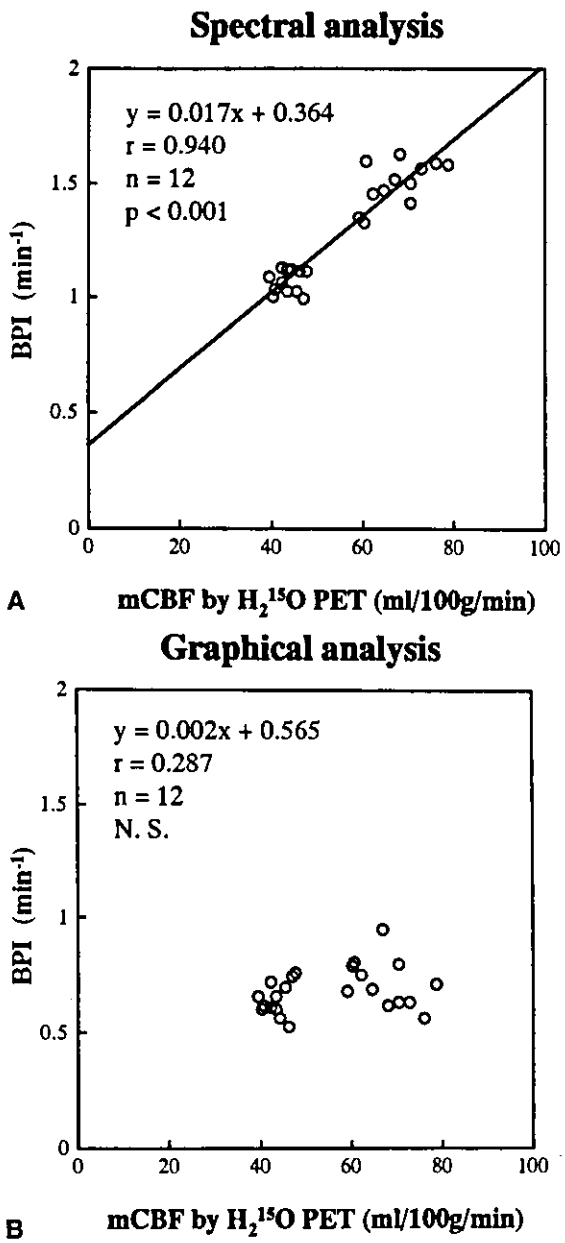

FIG. 2. Relationship between the brain perfusion index (BPI) values obtained by spectral analysis (BPI^S; **A**) and graphical analysis (BPI^G; **B**) using ^{99m}Tc-HMPAO (y) and the cerebral blood flow values measured using H_2O positron emission tomography (PET) ($mCBF^{PET}$) (x). Although the correlation between the BPI^S and $mCBF^{PET}$ values was statistically significant ($P < 0.001$), the correlation between BPI^G and $mCBF^{PET}$ was not. N.S., not significant.

DISCUSSION

^{99m}Tc-HMPAO is widely used as a radiotracer for the evaluation of brain perfusion and has been used to examine a variety of brain diseases, providing a "snapshot" of cerebral perfusion at the moment of administration (Nowotnik et al., 1985; Hayashida et al., 1993; Takasawa et al., 2000). The largest advantage of this tracer is its ability to capture acute events, even in emergency cases (Shimosegawa et al., 1994), since it is available in the form of a ^{99m}Tc-labeled kit. One of its drawbacks, however, is that its rate of uptake in the brain is greatly affected by the extraction fraction and retention fraction, especially when the CBF is elevated (Murase et al., 1992). This property must be considered whenever a brain study involving a quantitative analysis with ^{99m}Tc-HMPAO is performed.

Matsuda et al. (1992) reported a quantitative method of measuring CBF using ^{99m}Tc-HMPAO. This procedure can be used to noninvasively determine the BPI using radionuclide angiographic data (Fig. 1). The regional tracer uptake pattern obtained by a subsequent SPECT measurement can then be converted into an absolute regional perfusion map, after calibration, and superimposed on the derived hemispheric CBF data, using the appropriate tracer linearity correction. In essence, this calculation of regional CBF from the BPI is based on the linearization algorithm of Lassen et al. (1988) and yields a curve–linear relationship between brain activity and blood flow. However, since the BPI obtained by means of GA is derived from the slope of Gjedde-Patlak plot (Matsuda et al., 1992, 1995), which is proportional to the product of the first-pass extraction fraction of the tracer, retention fraction, and the CBF, it does not accurately reflect CBF, especially when the CBF is elevated, such as after the administration of acetazolamide (Murase et al., 1999).

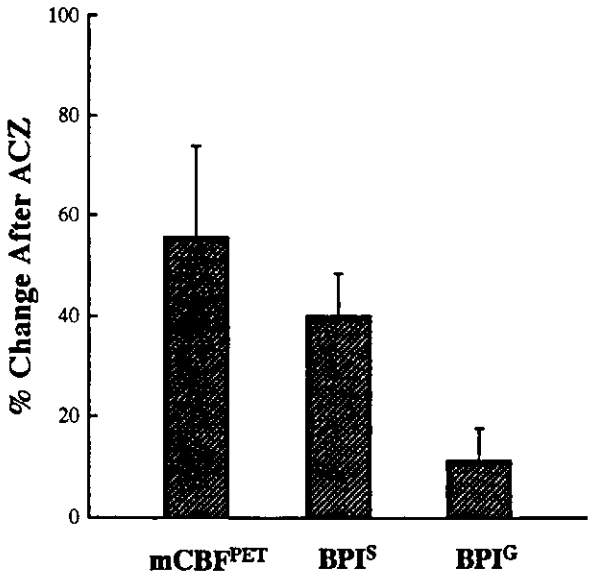

FIG. 3. Comparison between the degrees of increase in brain perfusion index (BPI) (percent change in BPI) and H_2O positron emission tomography (PET) ($mCBF^{PET}$) after the administration of 1g of acetazolamide (ACZ). The percentage change of spectral analysis–calculated BPI values (BPI^S) was significantly larger than that of graphical analysis–calculated BPI values (BPI^G) (Wilcoxon signed rank test).

SA has been previously used to analyze dynamic PET scans in humans; this technique provides data representing the time course of activity in tissue regions of interest and in arterial blood following the administration of a radiolabeled tracer (Cunningham and Jones, 1993). SA provides a simple spectrum of kinetic components that relates the tissue's response to the blood activity curve, facilitating the interpretation of dynamic PET data and simplifying comparisons between regions and subjects.

Murase et al. (1999) were the first to apply the SA method to SPECT data. They demonstrated two crucial advantages to estimating the BPI using SA. First, BPI^S is barely affected by the conversion of lipophilic, diffusible tracers to hydrophilic, nondiffusible tracers in the arterial blood of the brain. Since the influence of this phenomenon when ^{99m}Tc-HMPAO is used in humans results in at most a 1.0% difference in BPI, this phenomenon is probably negligible for technetium-99m-labeled compounds when the BPI is measured using SA. Second, the BPI is theoretically unaffected by the first-pass extraction fraction and retention fraction when measured using SA [see Appendix 2]. The assumptions underlying this analysis are based only on the linear model.

We studied the changes in BPI after the injection of acetazolamide in six healthy volunteers (Fig. 3). The results showed that the percent increase in BPI^G (11.3 ± 6.5%) was significantly lower than that in BPI^S (40.1 ± 8.4%). The extraction fraction and retention fraction decrease with increasing blood flow (Murase et al., 1992). This probably explains why the GA method gives an underestimation of flow in comparison with SA when flow is high.

The kinetic behavior of diffusible tracers, such as ^{15}O-labeled water, is crucially different from tracers that are trapped, such as ^{99m}Tc-HMPAO; thus, the distribution of ^{15}O-labeled water examined using PET reflects the CBF more reliably and is widely used clinically (Hayashida et al., 1996; Kuwabara et al., 1998). The percentage change in $mCBF^{PET}$ was 55.6%, significantly higher than that in BPI^S (Fig. 3). Furthermore, although the BPI^S and $mCBF^{PET}$ values were significantly correlated, y-intercept of the regression equation was somewhat large (Fig. 2A). As shown in Appendix 2, the BPI^S given by Eq. 3 is theoretically proportional to CBF. However, when the intravascular component is neglected, the sum of the α_i values becomes equal to the influx rate constant of the tracer, that is, K_1 (Cunningham and Jones, 1993), which is the product of CBF and the first-pass extraction fraction. When the temporal and spatial resolution for analysis are finite as in this study, the intravascular and extravascular components might not be separated adequately in SA, and then the BPI^S values obtained in this study might have been affected by the limited first-pass extraction fraction. This would be the main reason for the aforementioned findings shown in Figs. 2 and 3. As shown in Fig. 2, however, the significant relationship between $mCBF^{PET}$ and BPI^S can be used to estimate the percentage change in the absolute CBF after the administration of acetazolamide using BPI^S.

Acetazolamide is generally used to estimate the vascular reserve and/or to detect areas of misery perfusion (Kuroda et al., 2001; Vernieri et al., 1999). Reactivity to acetazolamide in patients with major artery occlusion identifies patients with high risk of subsequent ischemic stroke (Kuroda et al., 2001; Webster et al., 1995; Yonas et al., 1993). Thus, it is important to study the absolute CBF and the reactivity to acetazolamide in routine clinical settings, especially in patients with major artery occlusion. The significant correlation between BPI^S and $mCBF^{PET}$ found in this study suggests that CBF measurements obtained using SA might be as applicable as $H_2{}^{15}O$ PET measurements in clinical practice. We previously described the split dose ^{123}I-IMP SPECT method, which enables measurements of CBF to be obtained both at rest and after the administration of acetazolamide in a short time (Hashikawa et al., 1994). In the future, the split-dose method using SA will be used in clinical practice, and this novel, noninvasive method should be less troublesome to patients undergoing quantitative CBF examinations.

In conclusion, we have demonstrated a simple, useful, noninvasive method for the quantitative evaluation of CBF. Our results suggest that this novel SA method provides more reliable BPI measurements than the conventional procedure using GA for the quantification of CBF using ^{99m}Tc-HMPAO. The SA method may allow noninvasive absolute CBF quantification using ^{99m}Tc-HMPAO to be performed in routine clinical settings.

APPENDIX 1

Derivation of Eq. 2

When deriving Eq. 2, we replaced $C_a(t)$ in Eq. 1 by $S \cdot \delta(t)$, where S and $\delta(t)$ denote the scale factor and Dirac's delta function, respectively. The scale factor [S] was given by

$$S = \int_{-\infty}^{\infty} C_a(t)dt \qquad \text{(A1)}$$

Then, Eq. 1 became

$$C^S(t) = S \cdot \sum_{i=0}^{k} \alpha_i \cdot e^{-\beta_i t} \qquad \text{(A2)}$$

The tissue impulse response function [IRF^S (t)] was defined as

$$IRF^S(t) = \frac{C^S(t)}{S} = \sum_{i=0}^{k} \alpha_i \cdot e^{-\beta_i t} \qquad \text{(A3)}$$

yielding Eq. 2.

APPENDIX 2

Tissue impulse response function value at time zero

Blood flow (F) can be determined from the value of tissue impulse response function [IRF^S (t)] at time zero in the following fashion. The concentration of a tracer within a tissue at time t [$C_{tissue}(t)$] is determined from Fick's principle as

$$C_{tissue}(t) = \int_{-\infty}^{t} F[C_{in}(u) - C_{out}(u)]du \qquad (A4)$$

assuming that the system describing the flow of tracer into and through the tissue is linear and stationary (Gobbel and Fike, 1994). In Eq. A4, $C_{in}(t)$ and $C_{out}(t)$ represent the concentration of the tracer within the blood flowing into and out of the tissue, respectively.

If the input into the system is instantaneous and occurs at time zero, then $C_{tissue}(t)$ can be replaced by $S \cdot IRF(t)$ and $C_{in}(t)$ by Dirac's delta function multiplied by S [$S \cdot \delta(t)$], with S being the scale factor given by

$$S = \int_{-\infty}^{\infty} C_{in}(t)dt \qquad (A5)$$

Thus, IRF(t) is given by

$$IRF(t) = \int_{-\infty}^{t} F\left[\delta(u) - \frac{C_{out}(u)}{S}\right] du \qquad (A6)$$

yielding

$$IRF(0) = F \qquad (A7)$$

This indicates that the BPI^S given by Eq. 3 is proportional to CBF.

Acknowledgments: We thank Mr. Y. Nakamura and the staff of the Department of Nuclear Medicine and the Cyclotron staff of Osaka University Medical School Hospital for their technical support in performing the studies, as well as Miss S. Imoto and Miss R. Morimoto for their administrative assistance.

REFERENCES

Baron JC (2001) Mapping the ischemic penumbra with PET: a new approach. *Brain* 124:2–4

Baron JC, Bousser MG, Rey A, Guillard A, Comar D, Castaigne P (1981) Reversal of focal "misery-perfusion syndrome" by extra-intracranial arterial bypass in hemodynamic cerebral ischemia. *Stroke* 12:454–459

Cunningham VJ, Jones T (1993) Spectral analysis of dynamic PET studies. *J Cereb Blood Flow Metab* 13:15–23

Gobbel GT, Fike JR (1994) A deconvolution method for evaluating indicator-dilution curves. *Phys Med Biol* 39:1833–1854

Hashikawa K, Matsumoto M, Moriwaki H, Oku N, Okazaki Y, Uehara T, Handa N, Kusuoka H, Kamada T, Nishimura T (1994) Split dose iodine-123-IMP SPECT: sequential quantitative regional cerebral blood flow change with pharmacological intervention. *J Nucl Med* 35:1226–1233

Hayashida K, Hirose Y, Kaminaga T, Ishida Y, Imakita S, Takamiya M, Yokota I, Nishimura T (1993) Detection of postural cerebral hypoperfusion with technetium-99m-HMPAO brain SPECT in patients with cerebrovascular disease. *J Nucl Med* 34:1931–1935

Hayashida K, Tanaka K, Hirose Y, Kume N, Iwama T, Miyake Y, Ishida Y, Matsuura H, Nishimura T (1996) Vasoreactive effect of acetazolamide as a function of time with sequential PET O15-water measurement. *Nucl Med Commun* 17:1047–1051

Hellman RS, Tikofsky RS (1990) An overview of the contributions of regional cerebral blood flow studies in cerebrovascular disease: is there a role for single photon emission computed tomography? *Semin Nucl Med* 20:303–324

Hirano T, Minematsu K, Hasegawa Y, Tanaka Y, Hayashida K, Yamaguchi T (1994) Acetazolamide reactivity on 123I-IMP single photon emission computed tomography in patients with major cerebral artery occlusive disease: correlation with positron emission tomography parameters. *J Cereb Blood Flow Metab* 14:763–770

Huang SC (1983) Quantitative measurement of local cerebral blood flow in humans by positron emission tomography and ^{15}O-water. *J Cereb Blood Flow Metab* 3:141–153

Kuroda S, Houkin K, Kamiyama H, Mitsumori K, Iwasaki Y, Abe H (2001) Long-term prognosis of medically treated patients with internal carotid or middle cerebral artery occlusion. *Stroke* 32:2110–2116

Kuwabara Y, Ichiya Y, Sasaki M, Yoshida T, Fukumura T, Masuda K, Fujii K, Fukui M (1998) PET evaluation of cerebral hemodynamics in occlusive cerebrovascular disease pre- and postsurgery. *J Nucl Med* 39:760–765

Lassen NA, Anderson AR, Friberg L, Paulson OB (1988) The retention of [^{99m}Tc]-L,D-HMPAO in the human brain after intracarotid bolus injection: a kinetic analysis. *J Cereb Blood Flow Metab* 8(suppl 1):S44–S51

Llacer J, Veklerov E, Baxter LR, Grafton ST, Griffeth LK, Hawkins RA, Hoh CK, Mazziotta JC, Hoffman EJ, Metz CE (1993) Results of a clinical receiver operating characteristic study comparing filtered backprojection and maximum likelihood estimator images in FDG PET studies. *J Nucl Med* 34:1198–1203

Marchal G, Benail K, Iglesias S, Vaider F, Derlon JM, Baron JC (1999) Voxel-based mapping of irreversible ischemic damage with PET in acute stroke. *Brain* 122:2387–2400

Matsuda H, Tsuji S, Shuke N, Sumiya H, Tonami N, Hisada K (1992) A quantitative approach to technetium-99m hexamethylpropylene amine oxime. *Eur J Nucl Med* 19:195–200

Matsuda H, Yagishita A, Tsuji S, Hisada K (1995) A quantitative approach to technetium-99m ethyl cysteinate dimer: a comparison with technetium-99m hexamethylpropylene amine oxime. *Eur J Nucl Med* 22:633–637

Murase K, Tanada S, Fujita H, Sasaki S, Hashimoto K (1992) Kinetic behavior of technetium-99m-HMPAO in human brain and quantification of cerebral blood flow using dynamic SPECT. *J Nucl Med* 33:135–143

Murase K, Inoue T, Fujioka H, Ishimaru Y, Akamune K, Yoshimoto Y, Mochizuki T, Ikezoe K (1999) An alternative approach to estimation of the brain perfusion index for measurement of cerebral blood flow using technetium-99m compounds. *Eur J Nucl Med* 26:1333–1339

Nariai T, Senda M, Ishii K, Wakabayashi S, Yokota T, Toyama H, Matsushima Y, Hirakawa K (1998) Posthyperventilatory steal response in chronic cerebral hemodynamic stress: a positron emission tomography study. *Stroke* 29:1281–1292

Nowotnik DK, Canning LR, Cumming SA (1985) Technetium-99m-HMPAO: a new radiopharmaceutical for imaging regional cerebral blood flow. *J Nucl Med Allied Sci* 29:208

Shimosegawa E, Hatazawa J, Inugami A, Fujita H, Ogawa T, Aizawa Y, Kanno I, Okudera T, Uemura K (1994) Cerebral infarction within six hours of onset: prediction of completed infarction with technetium-99m-HMPAO SPECT. *J Nucl Med* 35:1097–1103

Takasawa M, Watanabe M, Yuasa Y, Iiji O, Hashikawa K, Matsumoto M, Kinoshita K, Nukata T (2000) Transient patchy boundary zone hyperemia following TIA episode with deep hemispheric ischemia: serial HMPAO SPECT study. *J Neurol* 247:804–806

Vernieri F, Pasqualetti P, Passarelli F, Rossini PM, Silvestrini M (1999) Outcome of carotid artery occlusion is predicted by cerebrovascular reactivity. *Stroke* 30:593–598

Webster MW, Makaroun MS, Steed DL, Smith HA, Johnson DW, Yonas H (1995) Compromised cerebral blood flow reactivity is a predictor of stroke in patients with systematic carotid artery occlusive disease. *J Vasc Surg* 21:338–345

Yonas H, Smith HA, Durham SR, Pentheny SL, Johnson DW (1993) Increased stroke risk predicted by compromised cerebral blood flow reactivity. *J Neurosurg* 79:483–489

AJNR Am J Neuroradiol 23:189–193, February 2002

Prognostic Value of Subacute Crossed Cerebellar Diaschisis: Single-Photon Emission CT Study in Patients with Middle Cerebral Artery Territory Infarct

Masashi Takasawa, Manabu Watanabe, Shiro Yamamoto, Taku Hoshi, Tsutomu Sasaki, Kazuo Hashikawa, Masayasu Matsumoto, and Naokazu Kinoshita

BACKGROUND AND PURPOSE: **Although chronic-stage crossed cerebellar diaschisis (CCD) is reported to be associated with the neurologic state or clinical improvement after infarct, the prognostic value of early-stage CCD remains controversial. Our aim was to determine whether measurements of CCD in the acute and subacute stages obtained at single-photon emission CT (SPECT) facilitate the prediction of stroke outcome.**

METHODS: **The pattern of cerebral blood flow changes after the occurrence of acute middle cerebral artery ischemia with severe cortical symptoms was examined by using technetium 99m–hexamethylpropyleneamine oxime (^{99m}Tc-HMPAO) SPECT. Fifteen patients (mean age, 73 years ± 8 [SD]) with unilateral ischemia were examined in the early subacute stage (10 days ± 5). In 11 patients, SPECT was performed in both the acute (16 hours ± 10) and subacute stages. From the total counts obtained from each cerebellar hemisphere, the asymmetry index (AI) was calculated as follows: [(value in unaffected hemisphere − value in affected hemisphere)/value in unaffected hemisphere] × 100. Clinical outcome (at 60 days) was assessed by means of the Scandinavian Stroke Scale (SSS) and Barthel Index (BI).**

RESULTS: **AIs in the acute stage and clinical outcome (ie, SSS and BI scores) showed no significant correlation, but the severity of AI in the early subacute stage correlated significantly with both the final SSS ($r = -0.69$; $P < .01$) and BI scores ($r = -0.82$; $P < .01$).**

CONCLUSION: **Cerebellar hypoperfusion detected at ^{99m}Tc-HMPAO SPECT in the early subacute stage in patients with supratentorial infarct indicates a worse clinical outcome.**

Baron et al (1) first demonstrated crossed cerebellar diaschisis (CCD) in patients with supratentorial infarction by using a noninvasive ^{15}O continuous inhalation technique coupled with positron emission tomography (PET). Previous studies demonstrated that CCD matched depression of blood flow and metabolism in the cerebellum contralateral to a supratentorial focal lesion, as detected with PET (1–4). The mechanism underlying CCD reportedly consists of interruption of the cerebropontocerebellar pathway that causes deafferentation and transneural metabolic depression of the contralateral cerebellar hemisphere (1–4).

CCD in the chronic stage is associated with neurologic improvement after infarct in the middle cerebral artery (MCA) territory (5, 6). Some investigators have reported that CCD appears to be prominent in patients with severe hemiparesis in various stages (1, 4). Recent studies showed that CCD in the acute stage is not predictive of neurologic outcome, as quantified with stroke scales for PET (5) or technetium 99m–hexamethylpropyleneamine oxime (^{99m}Tc-HMPAO) single-photon emission CT (SPECT) (7, 8). However, to our knowledge, no detailed reports about the predictive value of CCD at stages between the acute and chronic stages have been published.

We performed ^{99m}Tc-HMPAO SPECT in patients in the acute and subacute stages of MCA ischemia who presented with severe cortical symptoms. Our aim was to determine whether CCD in the acute and

Received February 22, 2001; accepted after revision September 26.

From the Division of Strokology, Departments of Cardiovascular Medicine and Clinical Research, Osaka-Minami National Hospital, Japan (M.T., M.W., S.Y., T.H., T.S. N.K.); and the Department of Nuclear Medicine (K.H.) and Division of Strokology, Department of Internal Medicine and Therapeutics (M.M.), Osaka University Graduate School of Medicine, Japan.

Address reprint requests to Masashi Takasawa, MD, Division of Strokology, Department of Internal Medicine and Therapeutics, Osaka University Graduate School of Medicine. 2–2, Yamadaoka, Suita City, Osaka, 565-0871, Japan.

© American Society of Neuroradiology

TABLE 1: Clinical characteristics and cerebellar AI

Patient No./Age (y)/Sex	MCA Side	Infarct		AI	SSS		RI	BI at 60 Days
		Mechanism*	Topographyt		Acute	At 60 Days		
1/78/F	L	E	F, T, P, d	13.6	13	38	55.5	63
2/72/M	L	E	F, T, P	13.3	16	37	26.2	54
3/60/M	R	E	F, T, P	11.9	24	41	50.0	48
4/64/M	L	E	F, T, P, d	10.6	18	61	32.5	42
5/81/M	L	A	T, P	10.0	20	65	39.5	43
6/67/F	L	E	F, T, P	10.0	16	67	26.2	71
7/88/M	R	E	F, T, P	9.6	33	43	40.0	66
8/75/M	R	E	P	9.5	32	34	7.7	55
9/77/M	L	E	F, d	7.3	24	54	88.2	87
10/59/F	R	E	d	5.9	36	58	100	100
11/81/M	L	A	P, d	5.7	9	54	91.8	86
12/81/M	L	E	T, d	5.5	12	58	100	90
13/67/F	R	E	F, d	4.4	22	55	91.7	95
14/72/M	L	A	P, d	2.1	8	44	72.0	95
15/82/M	L	E	d	1.2	28	54	86.7	95

* A indicates atherothrombotic; E, embolic.

† d indicates deep MCA territory; F, frontal; P, parietal; T, temporal.

subacute stages, as measured with ^{99m}Tc-HMPAO SPECT, facilitates prediction of the outcome and clinical improvement of stroke accompanied by MCA territory infarct.

Methods

Subjects

We examined 15 consecutive patients (11 men and four women; age range, 59–88 years; mean age, 73 years ± 8 [SD]) with acute cortical infarction in the territory of the unilateral MCA (Table). Patients with hemispheric symptoms and persistent hemiparesis were selected. Twenty-six SPECT scans were obtained in 15 patients with stroke; these showed that cerebral hypoperfusion involved the left hemisphere in 10 patients and the right hemisphere in the other five. All patients underwent ^{99m}Tc-HMPAO SPECT in the early subacute stage after the stroke episode (10 days ± 5). In 11 patients, SPECT was performed within 48 hours after the onset (16 hours ± 10). None of the patients in this study had clinical symptoms or MR imaging findings suggestive of ischemic episodes in the vertebrobasilar territory; routine MR imaging findings did not suggest gross morphologic alterations in the cerebellum. No thrombolytic agents were administered to any of the patients (9), but routine medications, such as antiplatelet agents, antibiotics, and heparin, were allowed. Patients 5 and 11 received intravenous Argatroban, a thrombin inhibitor, in the acute stage. No recurrences of stroke were noted during the 60-day follow-up period. Patients with complications (eg, chronic heart failure) that affected the activities of daily living and neurologic improvement were excluded. All patients, or their relatives, gave informed consent to participate in this study.

SPECT Imaging Protocol

SPECT imaging was performed 10–20 minutes after the intravenous administration of 740 MBq of ^{99m}Tc-HMPAO by using a two-head rotating gamma camera interfaced with a dedicated computer system. Sixty images were acquired within 20 minutes, with a 128 × 128 matrix and a low-energy high-resolution collimator during a 180° rotation. The transaxial sections were reconstructed by means of filtered backprojection with a Butterworth filter. Each reconstructed section was corrected for tissue absorption by using Chang's method. An average of 20 SPECT image planes, 3.9 mm thick, were required to image the entire brain. All images were resectioned parallel to the orbitomeatal plane before analysis.

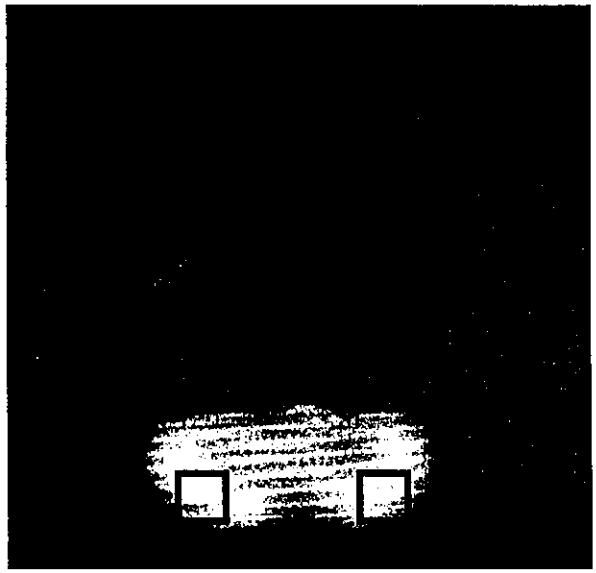

FIG 1. ROIs on a SPECT image of the cerebellum.

Image Analysis

The SPECT images were analyzed semiquantitatively. A 20 × 20-mm region of interest (ROI) was placed on the ipsilateral and contralateral cerebellar hemispheres (Fig 1) (10). From the total counts obtained from each cerebellar hemisphere, the asymmetry index (AI) was calculated by using the following equation: AI = [(value in unaffected hemisphere − value in affected hemisphere)/value in unaffected hemisphere] × 100.

Assessment of Patients' Neurologic Status

Clinical stroke severity was quantified at admission and at day 60 with the Scandinavian Stroke Scale (SSS) (scored from

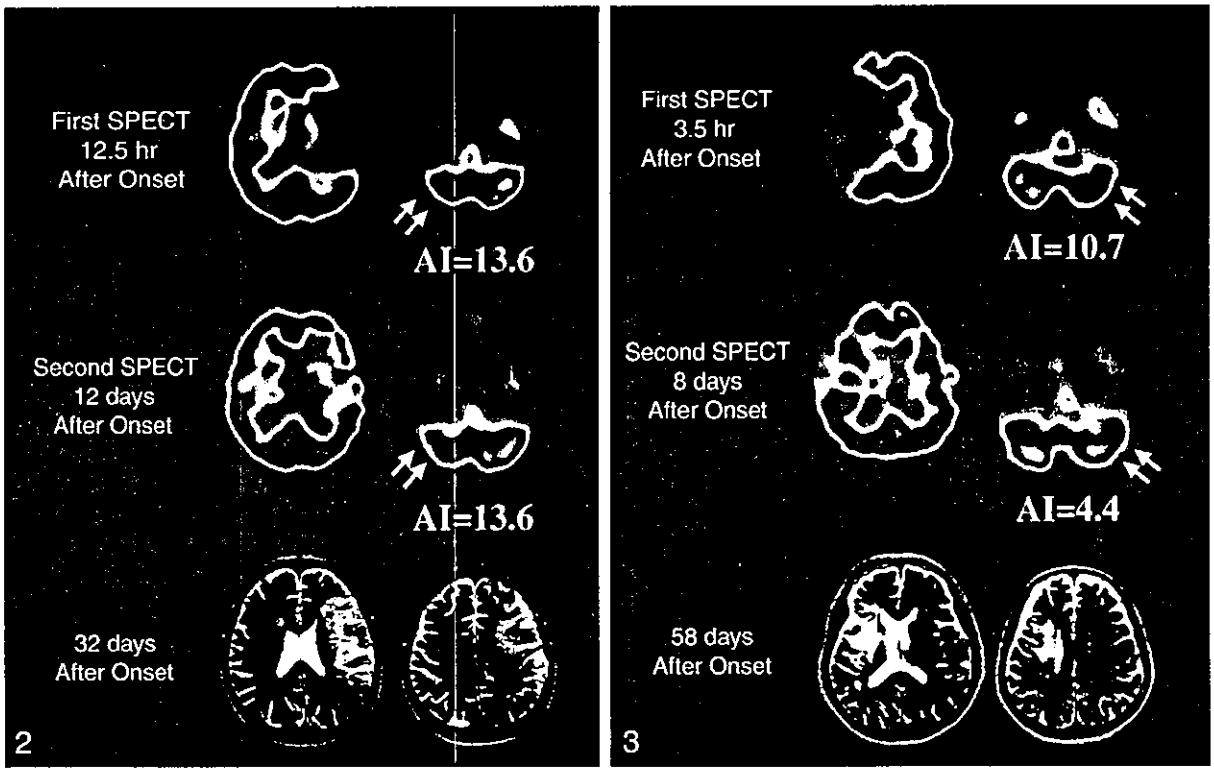

FIG 2. SPECT images obtained in patient 1 show severe cerebellar hypoperfusion (*arrows*) in both the acute (*top row*) and subacute (*middle row*) stages. This patient had SSS scores of 13 at admission and 38 at 60 days after onset. MR images (*bottom row*) obtained at 32 days show a large infarct in the left hemisphere.

FIG 3. SPECT images obtained in patient 13 show cerebellar hypoperfusion (*arrows*) in both the acute (*top row*) and subacute (*middle row*) stages. This patient had SSS scores of 22 at admission and 55 at 60 days after onset. MR images (*bottom row*) obtained at 58 days show an infarct in the right basal ganglia and frontal lobe.

0 to 58) (11). Functional assessment was performed at 60 days with the Barthel Index (BI) (scored from 0 to 100) (12). The recovery index (RI) was expressed as actual improvement, a percentage reflecting the proportion of potential improvement, as follows: RI = [(final SSS score at 60 days − initial SSS score)/(maximal SSS score − initial SSS score)] × 100 (13).

Statistical Analysis

Changes in AI or SSS were analyzed with the Wilcoxon signed rank sum test. Relationships between the degree of AI and clinical severity were evaluated with the nonparametric Spearman rank test. A P value of less than .05 was considered to indicate a statistically significant difference. Statistical analysis was performed with a statistical software package (SPSS for Macintosh).

Results

The degree of cerebellar hypoperfusion was calculated as the AI in the cerebellar hemispheres. The mean AI was 9.6 ± 1.2 (SE) (n = 11; range, 3.9–16.2) in the acute stage and 8.0 ± 1.0 (n = 15; range, 1.2–13.6) in the subacute stage. In 11 cases, both acute- and subacute-stage CCD measurements were available for evaluation of serial changes in cerebellar hypoperfusion. Results indicated that the mean AI of 9.6 ± 0.9 in the subacute stage was not statistically different from the value of 9.6 ± 1.2 in the acute stage (P = 0.86), although the time course of AI differed among patients (Figs 2 and 3).

The clinical data are summarized in the Table. Mean SSS scores improved from 21 ± 2 (SE) in the acute stage to 45 ± 2 at 60 days ($P < .01$).

First, we investigated the relationship between the AI in the acute stage and clinical outcome at 60 days and found no significant correlation between the first parameter and the final SSS score at 60 days ($r = -0.22$; $P = .49$), the final BI score at 60 days ($r = -0.04$, $P = 0.90$), or the RI ($r = -0.06$, $P = .85$). We also investigated the relation between AI in the subacute stage and clinical outcome at 60 days and found a good correlation with the final SSS score ($r = -0.69$; $P < .01$), the final BI score ($r = -0.82$; $P < .01$), and the RI ($r = -0.64$; $P < .05$) (Fig 4).

Discussion

The frequency of CCD has been reported to be higher in patients with infarcts involving the frontoparietal lobe, basal ganglia, and internal capsule at various stages (14, 15) than in other patients. Yamauchi et al (16) demonstrated that cerebral hemodynamic and metabolic status can cause CCD, even in small infarcts with unilateral major cerebral artery occlusion. However, little is known about the serial

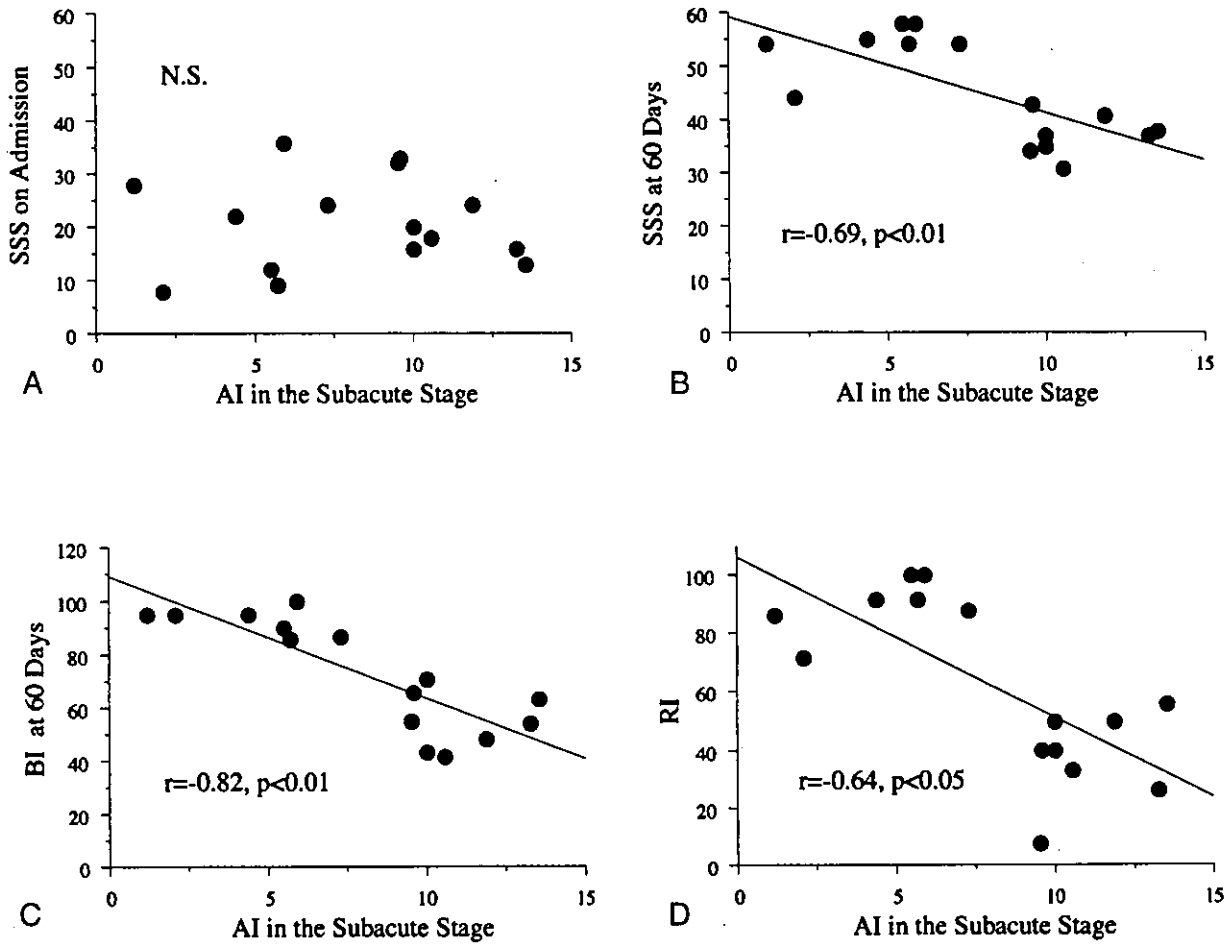

FIG 4. Relationships between the AI in the subacute stage and neurologic state. No significant (*N.S.*) correlations between the AI in the subacute stage and SSS score at admission were found (*top left*). AI in the subacute stage was significantly associated with the final SSS score at 60 days (*top right*), the final BI score at 60 days (*bottom left*), and the RI (*bottom right*), as the results of the nonparametric Spearman rank test indicate.

changes in cerebellar hypoperfusion or the prognostic value of CCD observed on ^{99m}Tc-HMPAO SPECT scans in infarct patients in the early stage.

Although the mean AI in the cerebellum did not significantly change from the acute stage to the subacute stage in the series as a whole, the time course of AI differed among patients. Infeld et al (7) found no statistically significant change in cerebellar hypoperfusion between the acute stage (within 36 hours after onset) and chronic stage (6.5 months ± 4), as assessed with ^{99m}Tc-HMPAO SPECT. Thus, our findings support their results.

In our study, the degree of AI in the acute stage was not significantly correlated with neurologic severity in the outcome stage. Infeld et al (7) demonstrated that CCD per se in the acute stage, as observed on ^{99m}Tc-HMPAO SPECT scans obtained within 72 hours of the onset, was not predictive of clinical outcome according to the Canadian Neurological Scale score or BI scores. Laloux et al (8) also reported that CCD in the acute stage, as determined with ^{99m}Tc-HMPAO SPECT (within 36 hours after onset), had no predictive value in terms of functional outcome, as assessed with the Rankin scale. Serrati et al (5) reported no significant correlation between contralateral cerebellar hypometabolism, (ie, oxygen consumption), as evaluated with early PET (within 30 hours after onset), and neurologic state at 60 days. Thus, our results are consistent with those of these three previous studies. At least two possible pathophysiologic explanations may account for our results in the acute stage. First, a reasonable speculation is that the still evolving cerebral perfusion and metabolic disturbances during the acute stage of cerebral infarction might have affected findings. Second, just after a stroke, CCD may still be in a pathophysiologically unsettled status, which can manifest itself as reversible damage and potential tissue recovery (5, 17, 18). Therefore, the degree of cerebellar hypoperfusion in the acute stage does not seem to have prognostic value regarding stroke outcome.

Reperfusion on ^{99m}Tc-HMPAO SPECT scans obtained during the subacute stage of ischemic stroke can mask supratentorial ischemic lesions (19–21), and thus, the severity or size of the area of supratentorial hypoperfusion may not be a predictor of stroke